MDPI

Review

A Review on the Nanofluids-PCMs Integrated Solutions for Solar Thermal Heat Transfer Enhancement Purposes

José Pereira *, Reinaldo Souza, António Moreira and Ana Moita

IN+ Center for Innovation, Technology and Policy Research, Instituto Superior Técnico, Universidade de Lisboa, Avenida Rovisco Pais, 1049-001 Lisboa, Portugal; reinaldo.souza@tecnico.ulisboa.pt (R.S.); aluismoreira@tecnico.ulisboa.pt (A.M.); anamoita@tecnico.ulsiboa.pt (A.M.)
* Correspondence: sochapereira@tecnico.ulisboa.pt

Abstract: The current review offers a critical survey on published studies concerning the simultaneous use of PCMs and nanofluids for solar thermal energy storage and conversion processes. Also, the main thermophysical properties of PCMs and nanofluids are discussed in detail. On one hand, the properties of these types of nanofluids are analyzed, as well as those of the general types of nanofluids, like the thermal conductivity and latent heat capacity. On the other hand, there are specific characteristics of PCMs like, for instance, the phase-change duration and the phase-change temperature. Moreover, the main improvement techniques in order for PCMs and nanofluids to be used in solar thermal applications are described in detail, including the inclusion of highly thermal conductive nanoparticles and other nanostructures in nano-enhanced PCMs and PCMs with extended surfaces, among others. Regarding those improvement techniques, it was found that, for instance, nanofluids can enhance the thermal conductivity of the base fluids by up to 100%. In addition, it was also reported that the simultaneous use of PCMs and nanofluids enhances the overall, thermal, and electrical efficiencies of solar thermal energy storage systems and photovoltaic-nano-enhanced PCM systems. Finally, the main limitations and guidelines are summarized for future research in the technological and research fields of nanofluids and PCMs.

Keywords: nanofluids; PCMs; heat transfer; thermal energy storage; photovoltaic/thermal systems

1. Introduction

The general usage of nanomaterials has been intensively studied in recent decades, given that these materials have considerable potential for scientific and technological progress and offer some beneficial features that can be closely related to the exploration of nanomaterials in different applications. Nanotechnology can be implemented in distinct technological areas, including IT technologies, innovative materials, biomedicine, and heat transfer enhancement, among many others. In particular, the energy field is one of the most appealing application vectors of nanotechnology, as nanomaterials may lead to remarkable advancements in diverse engineering applications.

Nanoparticles and their applications have been one of the main research topics because of the numerous potential fields of implementation. This review is focused mainly on the energy-related field since the addition of nanoparticles to base fluids to compose nanofluids and to phase-change materials to compose nano-enhanced phase-change materials and the corresponding applications in thermal energy storage and conversion processes will be relevant.

The employment of binary nanofluids for solar absorption cooling was reported by the authors Nourafkan et al. [1]. Their work analyzed the photo-thermal conversion efficiency under laboratory conditions with the utilization of a solar simulator. Hybrid nanoparticles with 50% wt. of lithium bromide were dispersed in 50% wt. of water. The results confirmed that the addition of the nanoparticles led to light-trapping efficiency enhancements and

consequently to an increase in the bulk temperature, ranging between 4.9% and 11.9%. Hence, the authors concluded that the nanoparticles used were very suitable for solar absorption cooling purposes.

In addition, the potential use of enhanced nanomaterials for thermoelectric generation was evaluated by the researchers Siddique et al. [2]. In their work, the Seebeck and Thomson effects of a nanostructured bulk alloy were determined with the addition of 0.1% vol. of silicon carbide nanoparticles, along with heat conduction capability and heat transfer loss into the surroundings. In view of the obtained results, it was confirmed that the inclusion of the silicon carbide nanoparticles increased the thermal efficiency to between 7.3% and 8.7%. Furthermore, the researchers Natividade et al. [3] studied the thermal efficiency of an evacuated tube solar collector system with a parabolic concentrator using a graphene nanofluid. The results demonstrated that the thermal efficiency of the solar collector increased from 31% to 76% with respect to that attained with the base fluid only.

Also, the usage of nanoparticles for photovoltaic/thermal purposes was investigated by the researchers Salem et al. [4]. In their work, the authors explored photovoltaic cell cooling with the enhancement of phase-change materials. In this direction, hybrid nanoparticles composed of an alumina phase-change material mixture were added to a water-based fluid in different concentration values. The obtained results revealed that it was possible to achieve a performance improvement in the delivered power output from the photovoltaic panel. The optimal concentration of the nanoparticles of 1% wt. provided the highest enhancement in the power output of the photovoltaic panel.

Also, the addition of silica nanoparticles to fatty acids was investigated by the researchers Martín et al. [5] to create a potential effective nano-enhanced phase-change material with increased thermal conductivity that is suitable for building applications. The experimental results confirmed that the addition of nanoparticles increased the thermal conductivity and heat transfer capability. The study also involved long-term performance experiments with cycling stability tests.

Additionally, the researchers Ren et al. [6] examined the phase-change material melting velocity for latent heat thermal energy storage, and the inclusion of nanoparticles was also analyzed. The results showed that the energy storage efficiency decreased with increasing volumetric concentration of nanoparticles, with the authors interpreting this result that way based on the enhanced viscosity and low energy storage capability of the phase-change material.

Balakin et al. [7] carried out an analysis of direct absorption collectors using the application of nanofluids. For this purpose, the authors conducted a computer fluid dynamics analysis in which the incorporation of nanoparticles induced an efficiency enhancement of the absorption collector by nearly 10%. In addition, the greatest collector performance enhancement was verified when magnetic nanoparticles were added, causing an increase in the efficiency of around 30%.

Bonab et al. [8] used aqueous copper oxide, aluminum oxide, and carbon nanotube nanofluids in a numeric simulation of a solar collector with absorbing pipes. The researchers reported that the thermal performance of the solar collector was enhanced with the incorporation of the nanoparticles in comparison to that of the one with water alone. The highest-efficiency enhancements were observed for concentrations inferior to 5% vol. in comparison to the ones obtained at higher concentrations.

Wang et al. [9] investigated the implementation of titanium nitride nanofluid as a plasmonic fluid in solar thermal applications. The obtained results showed that the titanium nitride nanofluid presented a superior photothermal conversion efficiency than those achieved with other commonly used nanofluids like, for example, carbon nanotubes or graphene, gold, or silver nanofluids.

A numerical analysis of the performance of gallium arsenide plasmonic solar cells with the addition of silver and gold nanoparticles was reported by the researchers Zhang et al. [10]. The research team verified that the incorporation of the nanoparticles enhanced the light absorption capability of the gallium arsenide solar cells. The highest increase in

the optical–electrical conversion efficiency was achieved with the inclusion of gold nanoparticles. It was noticed that, with the proper optimization of the nanoparticle properties, it was possible to reduce the thermalization losses and increase the electrical performance.

An experimental work focusing on the analysis of different factors that affect the thermal performance of flat-plate solar collectors was presented by the researchers Zayed et al. [11], with an assumed application of nanofluids. The obtained results confirmed that the most adequate nanoparticles in terms of energy/exergy were carbon-based ones. The efficiency of the system increased from 6.3% to 37.3% with respect to that attained with conventional nanofluids with concentration values of up to 2% wt.

Abdelrazik et al. [12] carried out an analytical study on the performance amelioration of hybrid photovoltaic/thermal solar collectors. In this sense, the authors added nanoparticles above the photovoltaic module and on the back side of the photovoltaic panel, together with a nano-enhanced phase-change material. The numerical simulation analysis revealed that the overall performance of the photovoltaic/thermal system decreased by approximately 6.7% with the incorporation of the nanoparticles. Nonetheless, in the case of the optical filtration above the photovoltaic panel, the efficiency of the system was enhanced by between 6% and 12%.

Innovative emulsions of paraffin waxes and water were experimentally evaluated by the authors Agresti et al. [13] with concentrations ranging from 2% to 10%, and the stability over time of the emulsions was investigated. According to the results, the melting heat was reduced when compared to the base fluid; however, the thermal capacity improved by up to 40%.

The incorporation of organic nanoparticles in phase-change materials for thermal energy storage purposes was investigated by the authors Sheikholeslami et al. [14]. An external magnetic field was applied to the system, and in concentrations of up to 4% wt., a 14% decrease in the solidification time was verified. The application of the magnetic field over the nano-enhanced phase-change material was demonstrated to be a very effective option for considerably increasing the solidification in energy storage applications.

De Matteis et al. [15] examined nano-encapsulated phase-change materials as potential effective choices for thermal management purposes for residential buildings. The research team found that the use of a nano-encapsulated phase-change material could decrease the heating/cooling energy requirements in residential buildings to between 1% and nearly 4%. The toxicity of the proposed solution was also investigated, and no harmful effects were detected with respect to human exposure.

The previous briefly addressed research works proved the importance of nanotechnology in various engineering applications. The review presented herein mostly deals with the experimental research dealing with nano-enhanced fluid and nano-enhanced phase-change materials. Therefore, the current contribution investigates both types of materials. A detailed literature review of nanofluid phase-change materials integrating photovoltaic/thermal systems is carried out in the current review paper, which is anticipated to provide useful insights for the researcher community.

This review paper addresses advanced nanofluid phase-change materials integrated into photovoltaic/thermal systems and principles from recently reported works. In addition, the design, operation, and research findings of different types of photovoltaic/thermal systems are also addressed. Figure 1 schematically illustrates the overview methodology used in the present study.

The primary selection was obtained with respect to the targeted keywords. The subject area was limited to energy, science, and technology and to nanofluids and phase-change materials. Articles written in English with the year of publication between 2000 and 2023 were selected. After the primary selection, the scientific articles discussing nanofluids and phase-change materials were subjected to secondary selection, where the main objective was to group the papers considering the areas of renewable energy, heat transfer, and solar thermal energy storage and conversion.
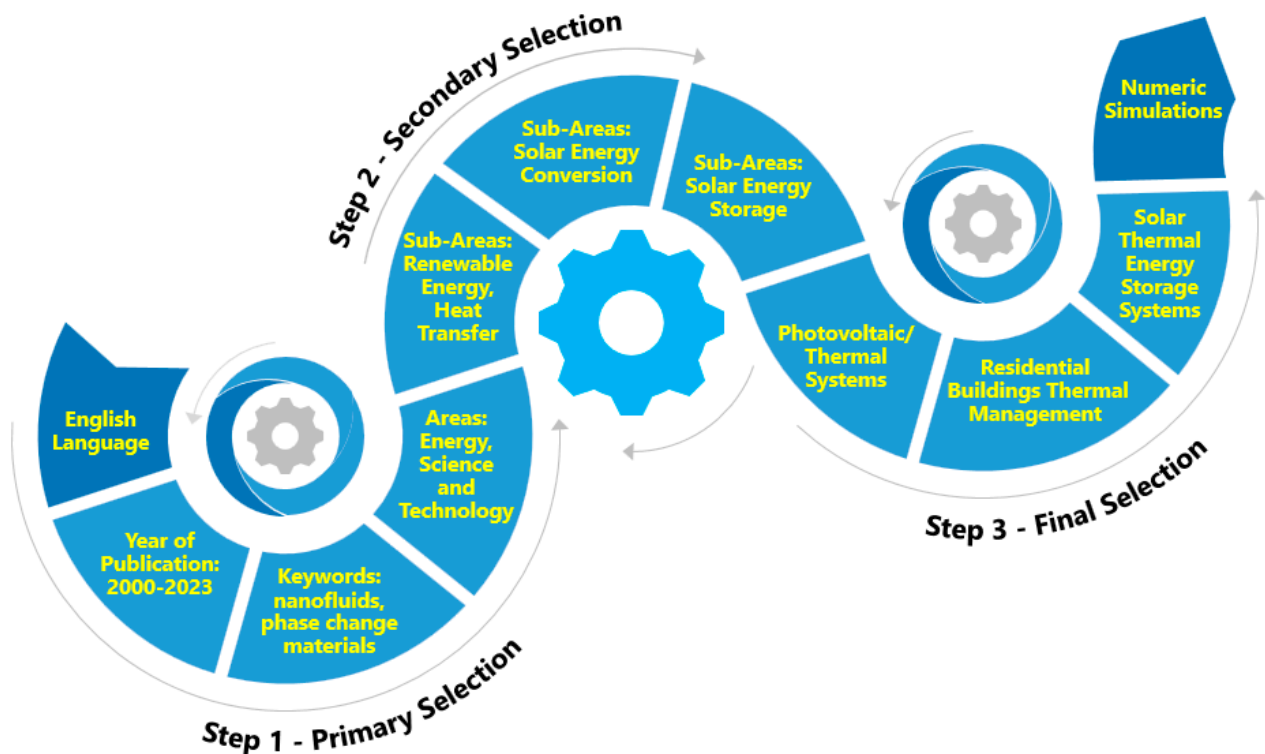
Overview Methodology

Figure 1. Schematic representation of the overview methodology followed in this work.

The final selection was carried out based on the combined exploration of the final solar thermal energy applications of nanofluids and phase-change materials. Therefore, it was not possible to describe each individual paper with respect to the specific applications, preparation techniques, and thermophysical property characterization. Instead, each article was classified with respect to the focus of its content considering the application, synthesis routes, and thermophysical characteristics. Depending on the specific selection criteria, some papers were addressed in multiple groups, based on the general content of the paper and the specific research findings.

The highest increase in interest regarding the released publications was in the period between 2015 and 2023 in the field of phase-change materials enhanced with nanoparticles in an amount superior to 100%.

The second highest increase in publications was in the case of energy storage applications in an amount of more than 90% from 2015 to 2023. In any case, the interest of the research community in nanotechnology applications is still progressing. The benefits related to the combined usage of nanofluids and phase-change materials and the addition of nanoparticles to these materials are remarkable and often closely related to the improvement of the performance of diverse systems, devices, and procedures. Nonetheless, the nature, size, and amount of the incorporated nanoparticles together with the preparation methods are the fundamental influencing factors. Since the potential implementation areas of nanoparticles are rather broad, this review focused on the simultaneous use of nanofluids and phase-change materials. Regarding the application area, the energy field was the focus of the review.

Also, the present work provides some guidelines for researchers dealing with phase-change materials, providing useful insights into the potential applications of combined nanofluids and phase-change materials. Figure 2 summarizes the main passive and active cooling techniques for the thermal management of photovoltaic/thermal systems.
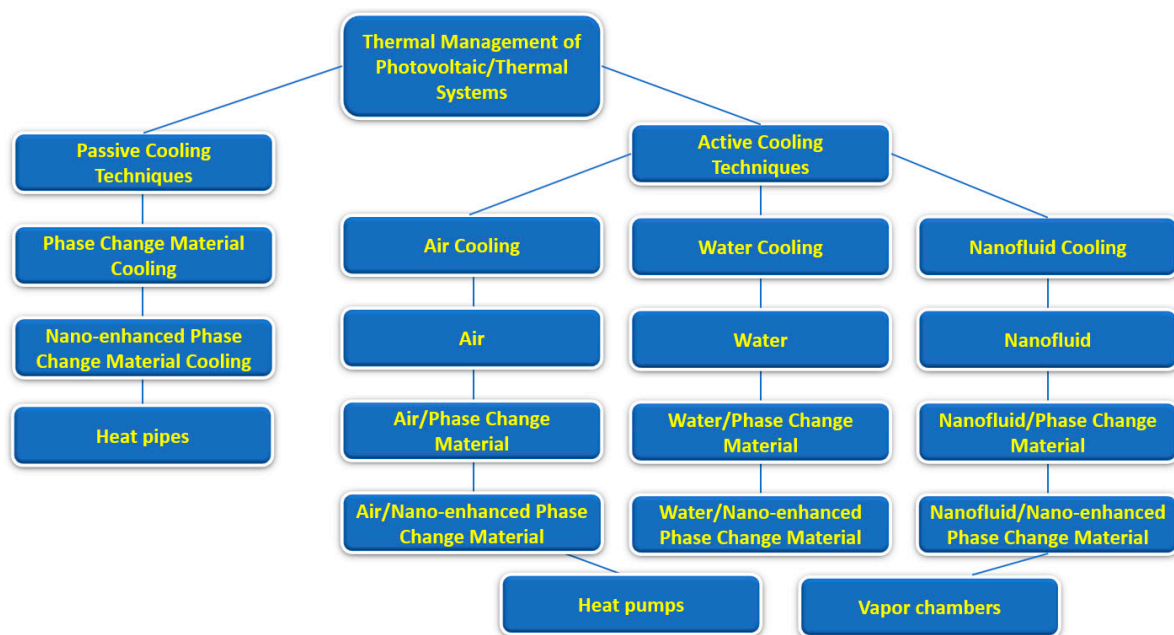
Figure 2. Main passive and active cooling techniques for photovoltaic/thermal systems.

2. Preparation Methodologies for Nanofluids

Nanofluids are normally employed as heat transfer fluids and thermal energy storage media. They also can be used as PCMs, and that is the case, for instance, for aqueous-based nanofluids. The nanofluids are synthesized through the dispersion of nanoparticles in a base fluid. First, a uniform and stable dispersion of nanoparticles is a critical issue concerning the stability over time of nanofluids. Consequently, there are several commonly followed strategies to improve the stability of nanofluids, such as the addition of surfactants, the application of strong ultrasonic force to break up the usual clustering of nanoparticles, and surface modification of nanoparticles. The one-step and two-step approaches are the main methods to produce nanofluids. Nonetheless, the emerging chemical processes are promising alternative methods of synthesis. In the one-step method, the procedures inherent to the drying, transportation, storage, and dispersion of nanoparticles are eliminated. For example, nanofluids can be synthesized via the physical vapor deposition technique, in which evaporation and condensation are conducted directly in the base fluid. This methodology prepares a stable nanofluid with uniform nanoparticles with comparatively low levels of aggregation and sedimentation over time. Nonetheless, the fundamental problems associated with the one-step method are the existence of residual reactants left in the nanofluids and the relatively high investment cost. On the other hand, the cost-effective two-step method is very suitable for the large-scale production of nanofluids. In this method, nanoparticles are prepared according to distinct methods and, after that, are dispersed into the base fluids. The main associated limitation is the usual aggregation of the incorporated nanoparticles in the base fluid. To overcome such a drawback and to improve the stability over time of the nanofluid, the addition of a surfactant is often explored. Figure 3 schematically represents a typical two-step method to produce nanofluids.

The following paragraph briefly describes some examples of the possible nanofluid synthesis routes. For instance, the researchers Altohamy et al. [16] dispersed nanoparticles of gamma alumina in water and studied the cool storage behavior of this water-based nano-enhanced PCM. The nanoparticles were added in concentrations of 0.5% vol. to 2% vol. The mixing was conducted by means of a sonicator at 30 °C for 90 min. Moreover, the authors Shao et al. [17] investigated the solidification behavior of hybrid nanofluids with titanium oxide nanotubes and nanoplatelets. Hybrid nanofluids with different titanium nanoparticle percentages and titanium oxide concentrations of 0.1% wt. to 0.3% wt. were prepared. The nanofluids were based on deionized water that was mixed for 30 min with nanomaterials

using firstly a magnetic stirrer and then an ultrasonic cleaner. It is not clear whether the 30 min period refers to a magnetic stirrer or an ultrasonic cleaner, nor is it indicated at which temperature, revolutions, and frequency the mixing was performed. The main research findings showed that different parameters affected the thermo-physical characteristics of the nanofluids and the mixing process. The size and shape of the nanoparticles were found to be critical, as was the sonication stage. It was also found that size and shape were mostly dependent on the preparation of the nanoparticles. The stability of the nanofluids was also affected by the surface charge, which was closely linked to the sonication step. It can be highlighted that the mixing process and the preparation of the nanoparticles were the most critical parameters and strongly affected the thermophysical properties of the nanofluids and their thermal stability and stability over time. Nanofluids present some disadvantages that have hindered their widespread use. Many of the discrepancies easily observed in the literature are related to differences in experimental results for the thermal conductivity of these mixtures [18]. An increase in thermal conductivity would be one of the main reasons for enhanced heat transfer in thermal systems. Although most researchers tend towards an increase in thermal conductivity with an increase in nanoparticle concentration, excess nanoparticles favor sedimentation and the formation of clusters in the base fluid. In thermal systems involving fluid flow, higher pumping energy may be required, especially in compact systems [19–21]. In these cases, in addition to stability-related issues, effects on viscosity and flow in channels with more complex geometries may suffer from clogging and pressure drops [22].
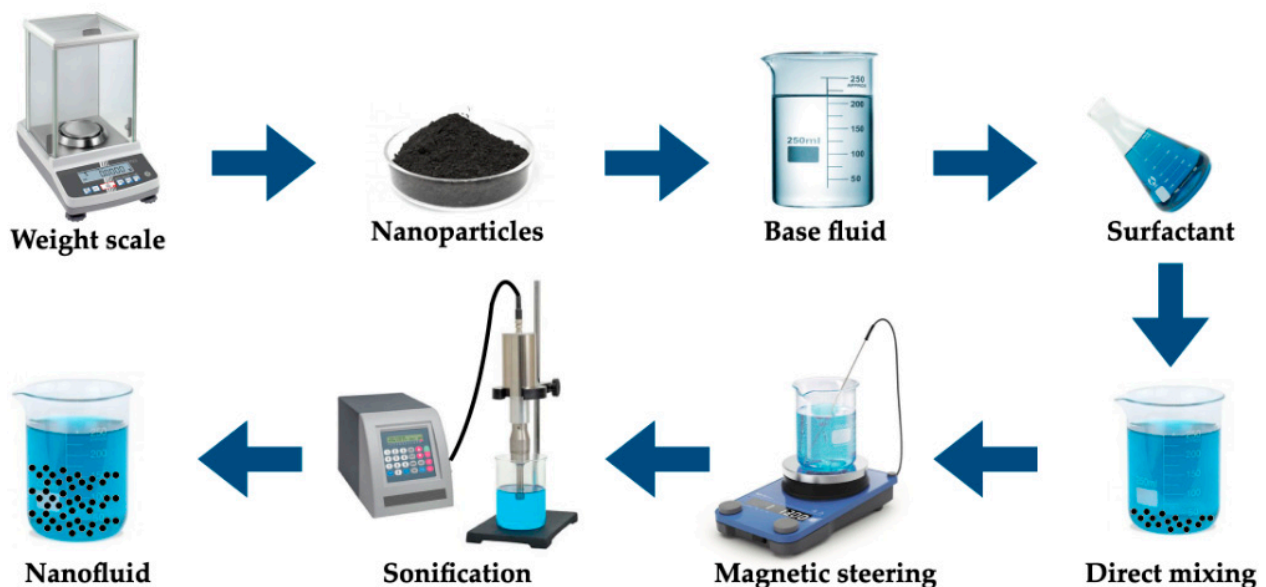

Figure 3. Typical two-step preparation method for nanofluids.

To overcome the problems related to long-term sedimentation, a series of techniques are employed, such as the use of stabilizing agents (surfactants), ultrasound, pH control, modification of the nanoparticle surface (such as size and shape), functionalization of the nanoparticles, and the use of different base fluids and concentrations of nanofluids in varying amounts. Surfactants act on the particle surface, preventing them from aggregating, which generally improves the wettability of the nanoparticles and reduces their surface tension [23].

The effect of nanoparticle size on nanofluids is still a highly controversial topic in the literature [21]. Whereas some authors argue that reducing the size of the nanoparticles increases the effective surface area for thermal exchange and intensifies the Brownian motion, resulting in an increase in thermal conductivity [24], other authors have reported a linear increase in conductivity with increasing particle size [18,25]. Ultrasound is part of the

so-called physical or mechanical methods, during which nanofluids are subjected to vibrations for a predetermined period to homogenize the mixtures and break up agglomerated nanoparticles or clusters, as they are commonly known as [26].

With proper pH control, nanoparticle agglomeration can be avoided, as particle electric charges are related to the pH of the medium, allowing for the alteration of repulsive and attractive forces between nanoparticles [27,28]. The functionalization of nanoparticles in nanofluids is a process that involves modifying nanoparticles with specific functional groups [21,29]. These functional groups aim to improve the stability, dispersion, and properties of the nanofluid according to its application. Furthermore, such modifications can increase the affinity of nanoparticles with the base fluid, promoting a more uniform dispersion and preventing long-term sedimentation.

Although the use of nanofluids may pose challenges, especially regarding long-term sedimentation due to the gain in thermal conductivity, interest in techniques to enhance stability and pursue better thermal properties of these colloidal mixtures has been intensifying.

Regarding the direct comparison between the two main preparation methods, it is noteworthy to mention the experimental work conducted by the authors Mohammadpoor et al. [30], who synthesized a copper–ethylene glycol nanofluid using different methods. The researchers compared the stability and heat transfer properties of nanofluids prepared by the one-step method and the two-step method. They confirmed that the nanofluid prepared with the one-step prepared was more stable without the incorporation of any stabilizer. They also verified that the single step nanofluid increased thermal conductivity by around 21%, whereas the two-step nanofluid increased it by 39.4% at a concentration of 0.01% wt. In general, the two-step method is preferred for the preparation of oxide nanoparticle nanofluids, whereas the one-step method is preferred for metal nanoparticles [31].

3. General Types and Characteristics of PCMs

The capability of storing substantial quantities of latent energy of between 100 MJ/m^3 and 250 MJ/m^3 and energy densities of from 150 MJ/m^3 to 430 MJ/m^3 for organic and inorganic PCMs [32], respectively, makes them very promising alternatives for thermal energy storage purposes. The increased latent heat capacity is the primary factor for a PCM to be applied in thermal energy storage applications. PCMs operate in narrow phase-change temperature ranges, which makes the evaluation of their suitability based on the operating temperatures and corresponding energy storage capacities. Figure 4 summarizes the main types of PCMs.
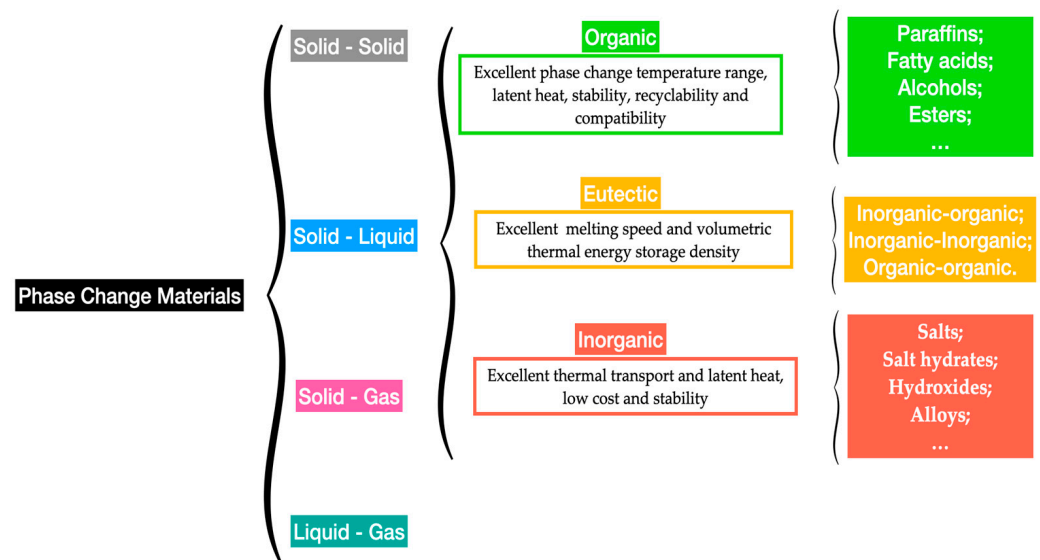

Figure 4. Main types of PCMs.

Nonetheless, PCMs possess relatively poor thermal conductivity, which is a limitation that negatively affects the charging rate of these materials. This thermal conductivity shortcoming is more noticeable in organic PCMs in comparison to inorganic PCMs [33]. Nevertheless, recent research efforts have been made to overcome such limitations by enhancing the thermal conductivity of PCMs. The transient hotwire method, transient plane-source method, laser flash method, and 3ω method are the most used thermal conductivity measurement techniques for PCMs. In the transient hotwire method, a hotwire is buried into solid, powder, or fluid samples, and the heat transfer process is initiated by a heating pulse from the hotwire to the sample. By monitoring the temperature response of the hotwire, the thermophysical parameters of the sample PCM can be rapidly acquired. Examples include multi-walled carbon nanotubes and graphene nanoparticles in stearic acid nano-enhanced PCMs [34]. Additionally, this method is also widely used for the measurement of PCM-based colloidal suspensions, including double-walled carbon nanotubes in palmitic acid [35] and carbon nanotubes in paraffin wax [36]. Nonetheless, the method poses some practical drawbacks, such as the damage inflicted on the internal structure of the samples, which is provoked by the insertion of the hotwire into them. Moreover, the transient plane-source method is also widely explored for the determination of the thermal conductivity of PCMs. The thermophysical features of the samples are detected through the heat flow from a plane-shape sensor. The sensor heats the samples and detects the heat flow rate, which is affected by the thermal transport ability of the sample PCMs. A relevant issue for the test structure is that both sides of the sensor must be in direct contact with the samples. In addition, the uniformity of the samples is also vital, given that the heating is one dimensional. For instance, the transient plane-source method measures the thermal conductivity of graphite nanoparticle nano-enhanced PCMs [37] and titanium oxide foam skeleton-reinforced PCMs [38]. As a practical restriction, this method makes it hard to determine with accuracy the thermal conductivity of uneven samples. Furthermore, the laser flash method is a non-contact method that heats PCM samples via a short energy pulse on one side of them. The thermophysical properties can be determined by measuring the temperature increase on the other side of the samples. On one hand, this method has the advantage of saving the sample preparation stages needed for contact measurement techniques, which may involve the risk of breaking up the internal structure of the samples. On the other hand, the method requires the use of uniformly opaque samples, small-width energy pulses, total absorption of the energy pulse by the illuminated side of the sample, and that there are only minor heat losses on the surface of the sample being analyzed. The laser flash method is mainly used to measure the thermal conductivity of bulk PCMs, such as, for example, aluminum–carbon nanoparticle paraffin wax PCMs [39] and expanded graphite–paraffin PCMs [40]. Additionally, the 3ω method uses a metal strip to heat the bulk material. The main beneficial feature is that a small sinusoidal current at angular frequency ω is fed into the metal strip, and the voltage response of the strip contains the first and third harmonics of the voltage, which improves the quality of the measurement of the thermophysical characteristics of the PCM. The 3ω method has the benefits of involving a minimized radiation effect and allowing for quick determination of the temperature dependence of the thermal conductivity over the steady-state method, although it usually takes more time than other measuring techniques. The 3ω method measures the thermal conductivity of PCMs in the form of nanopowders, bulk, coatings, fluids, and nanoparticles at an extended temperature range of between 10 K and 800 K. This method has also been employed, for instance, for the measurement of the thermal conductivity of adipic acid/sebacic acid–graphene nanoparticle PCMs [41] and multilayer film PCMs [42]. Moreover, the researchers Qiu et al. [43] proposed a freestanding sensor-based 3ω method with enhanced applicability to a broad range of dense and porous materials via non-destructive measurement and extraction of the thermal contact resistance. Urea formaldehyde paraffin PCM microcapsules were characterized with the freestanding sensor-based 3ω method. This measurement provided a reliable basis for the study of the thermal conduction mechanisms of PCM microcapsules. Figure 5 illustrates

the main measuring methods for the thermal conductivity of PCMs. Figure 6 summarizes the fundamental strategies for the thermal conductivity enhancement of PCMs. Most PCMs perform poorly in latent thermal energy systems due to their low thermal conductivity. PCMs' low thermal conductivity leads to a lower heat transfer rate from heat transfer fluid to PCMs. In consequence, it reduces the energy storage and release capacity of the latent thermal energy storage system and increases the time required for complete melting and solidification processes as well. To overcome this challenge, researchers have introduced new techniques, namely, extended surface, composites, multiple PCMs, and encapsulation, which are helpful for increasing the heat transfer rate between the heat transfer fluid and the PCM. As is known, during the melting process, convective heat transfer is dominant and conductive heat transfer vanishes as the process progresses, which is contrary to the solidification process. If fin configuration is used along with a PCM, it accelerates the melting and solidification processes by means of encouraging conductive heat transfer in both processes throughout. Numerical investigation on heat transfer enhancement of PCMs with a fin array system was studied for carrying out the effect of the fin pitch, the thickness of the module, the vertical/horizontal orientation of the modules, and the driving temperature gradient [44]. The obtained results indicated that a decrease in fin spacing caused a significant decrease in the amount of time required for complete melting for both horizontal and vertical modules. In addition, the authors Castell et al. [45] evaluated the heat transfer coefficient using external vertical fins and found that the vertical fins in PCM modules decreased the heat transfer coefficient more than the one attained with the PCM modules without any fins. But, in contrast, the exploration of vertical fins increased the heat transfer rate between the PCM and the heat transfer fluid because of the increased heat transfer area of the vertical fins. Also, the authors Nayak et al. [46] numerically evaluated the effectiveness of fins in improving the thermal conductivity of PCMs for cooling electronics. In view of the results, it was found that an increase in the number of fins used in the PCM increased the heat transfer rate. Nonetheless, beyond increasing a certain number of fins, there was no noticeable increase in the heat transfer rate. It was also found that rod-shaped fins performed better than plate-shaped fins, as they were able to maintain a better temperature distribution within the PCM. Moreover, the researchers Zhao et al. [47] inferred the thermal performance of PCMs embedded with metal foams experimentally and numerically. Compared to the results of the pure PCM, the effect of metal foams on the heat transfer rate was increased by up to 20 times and 10 times during the solidification and melting processes, respectively. Additionally, the heat transfer enhancement by metal beads was investigated for energy storage and release in single spheres during the solidification and melting of paraffin wax-enclosed spherical capsules [48]. The experiments were conducted as a function of the number and diameter of the metal beads. The combined thermal conductivity of the PCM and the metal beads increased significantly, thereby accelerating the heat transfer rate, which, in turn, provoked a decrease in the solidification and melting times. High-thermal-conductivity materials like graphite can be impregnated with PCMs with low thermal conductivity to achieve improved heat transfer features and phase-change performance of those PCMs. Furthermore, the authors Sari and Karaipekli [49] prepared palmitic acid and an expandable graphite composite to form a stable PCM via vacuum impregnation. The thermal conductivity of the form-stable composite of the palmitic acid-expandable graphite was 2.5 times higher than that of the pure palmitic acid of $0.17 \ \mathrm{Wm^{-1}K^{-1}}$. Also, the researchers Rao and Zhang [50] prepared graphite–paraffin nano-enhanced PCMs and found that, with higher weight concentrations of graphite, there was a decrease in the latent heat storage capability. For this reason, it was necessary to find the ideal concentration of graphite that would induce the maximum enhancement in the thermal conductivity of the PCM. Moreover, the researchers Wang et al. [51] synthesized a stearic acid–polymethylmethacrylate PCM for latent heat thermal storage purposes through ultraviolet curing dispersion polymerization. The melting and freezing temperatures and the latent heats of the stable form of the stearic acid–polymethylmethacrylate PCM were determined to be 60.4 °C and 50.6 °C and

92.1 J/g, and 95.9 J/g, respectively. Based on the obtained results, the authors concluded that nano-enhanced PCMs can be successfully explored as latent heat storage materials for passive solar building applications. In the multiple-PCM approach, the PCMs are usually arranged in order of decreasing melting points, maintaining an almost constant temperature difference during the melting process, even though the heat transfer fluid temperature decreases in the flow direction [52]. This leads to an almost constant heat flux to the PCM. During discharge, if the heat transfer fluid flow direction is just opposite to charging, then the PCMs remain in increasing order of their melting points. The overall energy efficiency can be enhanced by using multiple PCMs rather than only one PCM in a photovoltaic/thermal system. This research work can also help with determining the required number of PCMs and their respective melting point temperatures to improve system efficiency in the practical design of thermal storage systems. In another research work, similar work was carried out for multiple PCMs with fins in a latent heat storage unit [53]. The authors summarized that the multiple-PCM model resulted in a considerable amount of stored energy in the form of latent heat compared to the single-PCM model. A nearly uniform outlet temperature of the heat transfer fluid was obtained with the multiple-PCM latent heat storage modules compared to the single-PCM module. Moreover, the authors Shaikh and Lafdi [54] performed a numerical analysis on a combined diffusion and convection heat transfer in varied configurations of composite slabs employing multiple PCMs. It was observed that the total energy charge rate could be considerably enhanced by using composite PCMs compared to a single PCM. The authors Cui et al. [55] performed a numeric simulation carried out on a solar receiver thermal storage module operating with three different PCMs and a single PCM separately, in which the maximum heat transfer temperature, fluid outlet temperature, and liquid PCM fraction of the total heat transfer tube were obtained and compared with those attained with the single PCM. Compared with the single PCM, the multiple PCMs enhanced the energy rate, improving the performance of the receiver and profoundly decreasing the fluctuation of the fluid outlet temperature. Furthermore, in the PCM encapsulation method, micro-sized PCM particles are enclosed in a sphere or cylinder. The PCM inside the capsule is designated as the core and the solid capsule as the shell. The shell can be made of a wide range of materials, including natural and synthetic polymers. The encapsulation of PCMs can be performed chemically through, for instance, co-acervation, and physically through, for instance, spray drying. The authors Hawlader et al. [56] prepared an encapsulated paraffin wax and inferred its phase-change behavior during energy storage and release processes. Both complex coacervation and spray-drying methods were employed to prepare the encapsulated paraffin particles. The microcapsules had high energy storage and release capacities in the range of 145 to 240 J/g. Also, polymethylmethacrylate microcapsules containing n-octacosane as a phase-change material for thermal energy storage were investigated [57]. The melting and freezing points and the latent heats of the microencapsulated octacosane as a PCM were found to be 50.6 °C and 53.2 °C and 86.4 J/g and −88.5 J/g, respectively. In addition, thermal gravimetric analysis indicated that the microencapsulated octacosane had good chemical stability. It was understood that the prepared microencapsulated octacosane has good energy storage potential. Though the microencapsulated PCMs exhibited good energy storage and release capacities, it was not able to perform well under repeated cycling, even though the large particles of the microencapsulated PCM not only increased the viscosity of the fluid but were also often crushed during pumping. For this reason, it is necessary to prepare nano-encapsulated PCMs with smaller nanoparticle sizes of up to 150 nm.

Also, organic PCMs exhibit high flammability, tend to leak in the course of the melting process, and have low volumetric heat storage capabilities [58]. On the other hand, inorganic PCMs exhibit enhanced volumetric heat storage capacities [59], with metals and salt hydrates demonstrating improved thermal conductivity and latent heat capacities, making inorganic PCMs a very suitable choice, especially for applications in solar thermal energy systems and devices [60]. Nevertheless, these materials often present supercooling and

incongruent phase transitions. Figure 7 summarizes the fundamental beneficial features of PCMs that determine their selection for specific applications.
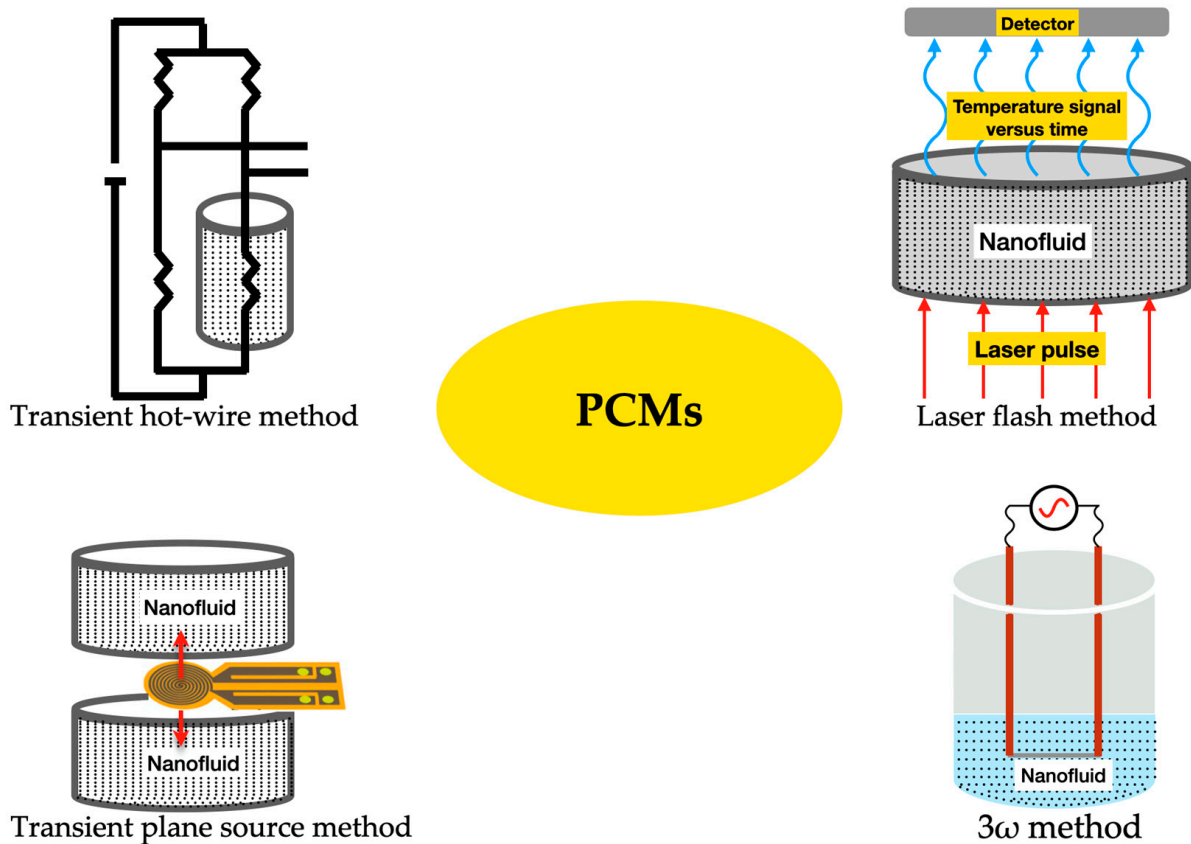

Figure 5. Main methods of measuring the thermal conductivity of PCMs.
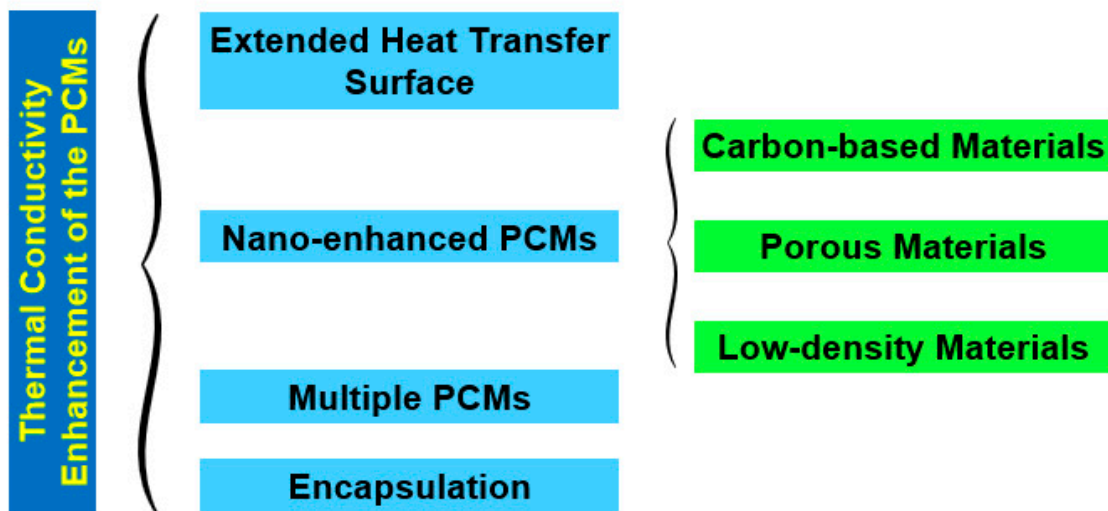

Figure 6. Main strategies for the enhancement of the thermal conductivity of PCMs.

Still concerning the beneficial features of PCMs, recently published research studies attempted to produce environmentally friendly PCMs [58]. These green PCMs are derived from bio-degradable and eco-friendly sources, including soya-oil, palm oil, and coconut oil [61]. The published research efforts in this field include the studies by the authors Boussaba et al. [62], who revealed that the exploration of palm kernel vegetable oil for thermal

energy management of residential buildings is feasible. The use of coconut oil was also suggested in [63] for air temperature regulation. Bio-based PCMs are highly promising yet are represented less in the literature compared to paraffin-based PCMs, and consequently, further studies on the exploration of eco-friendly PCMs for thermal energy storage applications are welcome. The solid–liquid type of PCMs is greatly employed in thermal energy storage systems because of their enhanced latent heat capacity and facile reversibility to either state during the charge and discharge processes [64]. Organic PCMs exhibit desirable latent heat of fusion, congruent fusion, thermal stability, minimal supercooling, recyclability, low toxicity, and thermal insulation due to their low thermal conductivity [65]. Organic PCMs are also compatible with the building materials and polymeric materials of latent heat storage tanks. Paraffins are organic PCMs with the general chemical formula C_xH_{2x+2}. They have a volumetric latent heat capacity of 179 MJ/m^3 and a thermal conductivity of 0.2 W/m °C [60]. Non-paraffin PCMs include esters, glycols, fatty acids, alcohols, and other organic PCMs. Inorganic PCMs include water, salts, hydrated salts, and metallic alloys in association with additives. The general form of salts is A_xB_y and the general form of hydrated salts is $A_uB_v \cdot n(H_2O)$, and they are widely studied for thermal energy storage purposes. In addition, inorganic PCMs often present significant heat of fusion per unit volume; better thermal conductivity than that of their organic counterparts, being twice that of paraffin-based PCMs; minimal volume change during phase change; non-flammability; compatibility with polymeric materials; and cost-effectiveness, making them very attractive options for thermal energy storage applications. The main problems associated with the use of inorganic PCMs are their supercooling effect, poor thermal stability, comparatively poor nucleation, and segregated phase change [66]. Also, it should be stated that the metallic alloy PCMs require further research work, since their elevated weight may hinder their applicability in thermal energy storage purposes [64]. On the other hand, eutectic mixtures are obtained from mixing two or more compounds, either organic or inorganic or both, such that they take on a suitable operating temperature [64]. The main benefits of eutectic mixtures comes from their high phase temperature for the intended application [59]. Eutectic mixtures also demonstrate increased enthalpy, do not undergo supercooling, and have congruent phase transition, unlike inorganic PCMs. Nonetheless, these mixtures are costly, at two or three times the price of their individual constituent PCMs. Hence, further studies should be conducted to overcome this price limitation, and the challenges of cost-effective feasibility and scalability of the exploration of eutectic mixture PCMs in energy storage applications should be better understood. It should be noted that the published literature in the field also covers the solid–gas and solid–solid classes. That is the case, for example, of the study performed by the authors Das et al. [67], who studied the application of liquid–gas PCMs in photovoltaic/thermal solar energy systems. Moreover, the researchers Kong et al. [68] studied the use of solid–solid PCMs for thermal energy storage purposes. The investigated PCMs exhibited a latent heat of 111.7 J/g and improved thermal stability. Also, the authors Du et al. [69] applied flame-retardant solid–solid phase-change composite nanosheets in solar thermal energy storage technology, resulting in enhancements of 88.5% and 69.4% in the energy efficiency and thermal conductivity, respectively. The current review pays special attention to the solid–liquid PCMs that absorb considerable thermal energy amounts during the melting process (charging stage) and release this energy during the solidification process when a cold inlet airstream is applied over it (discharging stage) [70]. Such practical characteristics are very suitable for thermal applications using the temperature changes between day and night. Many studies are completely focused on the general exploration of solid–liquid PCMs because of their improved properties in practical applications. Nonetheless, the gap still remains in overcoming their fundamental problems [71], hindering their best thermal performance potential in thermal energy storage systems.
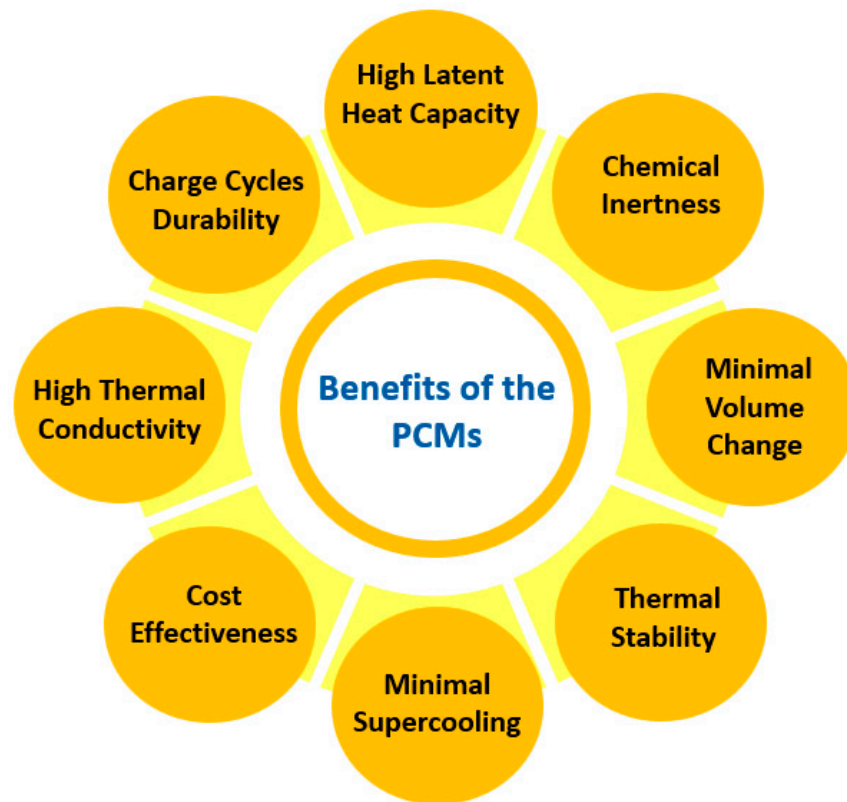
Figure 7. Fundamental benefits of PCMs.

4. Thermophysical Properties of Nanofluids and PCMs

4.1. Thermal Conductivity

The thermal conductivity of nanofluids depends on various factors like the type, morphology, and concentration of the added nanoparticles; the type of base fluid; the addition of surfactants; and the operating temperature. Nonetheless, the recent findings about their contribution to the effective thermal conductivity of nanofluids are inconsistent and often persist with some discrepancies and somewhat unexpected results. For example, the researchers Philip et al. [72] investigated thermal conductivity changes with a volumetric concentration of oleic acid-coated magnetite nanoparticles dispersed in kerosene-based fluid. No thermal conductivity increase was reported up to a concentration value of 1.7% vol. Beyond this value, the thermal conductivity of the developed nanofluid changed linearly with the concentration of nanoparticles. The authors stated that the thermal conductivity remained unchanged at low concentrations because of the uniformly dispersed nanoparticles, whereas at higher concentrations the existing nanoparticle clusters in the kerosene could have been the responsible for the verified thermal conductivity increase.

Chon et al. [73] evaluated the impact of nanoparticles added in the sizes of 11 nm, 47 nm, and 150 nm on the thermal conductivity of alumina aqueous nanofluids. The authors observed a greater thermal conductivity enhancement when they added the smaller nanoparticles of 11 nm. This was interpreted based on the enhanced Brownian motion of the smaller nanoparticles.

Beck et al. [74] found that the thermal conductivity of the nanofluids increased with increasing nanoparticle size. The research team argued that the verified thermal conductivity decrease for the smaller particles was caused by the enhanced phonon scattering at the interface between the nanoparticles and the base fluid. Indeed, when dealing with nanoparticle-based fluid suspensions, the actual size of the nanoparticles is their hydrodynamic size because of the contribution from the ordered liquid layer around the nanoparticles and the surfactant molecules around the surface of the dispersed nanoparticles.

Jeong et al. [75] studied the thermal conductivity of aqueous nanofluids containing zinc oxide nanoparticles with different morphologies and in different concentrations. The obtained results revealed a 12% increase in the thermal conductivity of the nanofluids with spherical nanoparticles, whereas the increase was of 18% when the authors added rectangular zinc oxide nanoparticles to water.

Murshed et al. [76] observed an increase in thermal conductivity of 17.5% with respect to that of ethylene glycol alone in the nanofluid composed of 5% vol. titanium oxide spherical nanoparticles dispersed in ethylene glycol-based fluid. The increase was of 20% when the same concentration of titanium oxide cylindrical nanoparticles was added. Also, the authors Zhu et al. [77] verified a higher thermal conductivity enhancement of 38% for iron oxide nanofluids than for titanium oxide, copper oxide, and alumina nanofluids (30% increase), though the thermal conductivity of the iron oxide of 7 W/mK was lower than that of the titanium oxide (11.7 W/mK), copper oxide (20 W/mK), and alumina (36 W/mK). The observed enhancement for Fe_3O_4-based nanofluid was attributed to the alignment of the nanoparticles as clusters, where the thermal conductivity increased with increasing concentration because of the increased length of the aligned particles.

Hong et al. [78] reported a higher thermal conductivity increase for iron nanofluids than for copper nanofluids, even though the bulk iron had a lower thermal conductivity of 80 W/mK than the bulk copper, of 384 W/mK. In fact, the iron nanofluids demonstrated an 18% increase in the thermal conductivity at a 0.55% vol. of nanoparticles, whereas the copper nanofluid at the same concentration value exhibited a 14% increase.

The last two studies demonstrated that, contrary to what was expected, the incorporation of highly thermal conductive nanoparticles is not always the best choice for enhancing the thermal conductivity of nanofluids. Instead, the wetting of the surface of the nanoparticles and the heat transfer capability at the solid–liquid interface are usually determining factors for the thermal conductivity enhancement verified in the nanofluids.

On the other hand, the researchers Dadwal et al. [79] examined the influence of the size of the nanoparticles on the thermal conductivity of magnetite nanoparticles suspended in kerosene and toluene. The researchers reported distinct tendencies of the thermal conductivity evolution with the size of the nanoparticles in the two base fluids, given that a thermal conductivity increase with increasing nanoparticle size was observed for the kerosene, whereas, with toluene as base fluid, the smaller nanoparticles promoted a thermal conductivity increase. The authors argued that the different evolutions of the size-dependent thermal conductivity could have been caused by the different nanoparticle-based-fluid interactions. The interaction between the nanoparticles and the molecules of the base fluid determines the thickness of the interfacial layer. This interaction is different for different base fluids, and it fundamentally decides the density of the nanolayer at the solid–liquid interface, which in turn affects the heat transfer performance at this interface.

Accordingly, the authors Kamalvand et al. [80] analyzed the enhancement in thermal conductivity of nanofluids with the adsorption of the molecules of the solvent onto the nanoparticles at distinct temperature values. The investigation team found a linear increase in thermal conductivity with the adsorption of the base fluid molecules onto the surface of the dispersed nanoparticles. Also, the authors confirmed that the adsorption level of the molecules of the base liquid increased with increasing bulk temperature.

Altan et al. [81] investigated the impact of the base fluid on the thermal conductivity of iron oxide nanoparticles coated with capric acid and oleic acid surfactants and suspended in hexane, heptane, and mineral oil. The research team verified a greater thermal conductivity increase when using hexane as the base fluid, followed by heptane and mineral oil. The researchers stated that the greater increase was not directly linked to the low thermal conductivity of the base fluid, and that, instead, the interactions between the base fluid and the added surfactant at the solid–liquid interface could be the main reason behind the thermal conductivity enhancement.

Shao et al. [17] evaluated an aqueous hybrid nanofluid containing nanoparticles of titanium oxide under the form of nanotubes of 9 nm to 10 nm and nanoplatelets of 50 nm

to 80 nm. It was confirmed that the nanofluid at 0.1% wt. of titanium oxide with 25% of titanium nanoparticles showed the greatest enhancement in thermal conductivity, of 22.3%, in comparison to that of the water-based fluid. The impact of the super-cooling degree of the hybrid nanofluids decreased by up to 4.97 ± 0.2 °C and 5.27 ± 0.2 °C, respectively, compared to mono nanofluids. The freezing time for the hybrid nanofluid was also diminished by up to 54.9% in comparison to the titanium nanoplatelet nanofluid and by 56.4% compared with the nanofluid with titanium nanoparticles. Concerning the thermal conductivity of the phase-change materials with the incorporation of nanoparticles, it can be stated that most of the available papers on the subject focus on thermal conductivity enhancement as a direct effect of the addition of nanomaterials to phase-change materials.

The only exception was the study conducted by Colla et al. [82], where the addition of alumina nanoparticles to paraffin caused a 7–8% lower thermal conductivity compared with that of pure paraffin. There is no clear explanation for this phenomenon in the mentioned study. Generally, due to the improved thermal conductivity of nanocomposites and nanofluids, a reduction in heating, melting, and solidification times can be expected. Usually, the expected improvement in thermal conductivity is in the range of 20–100%, but there are examples of even higher improvements being reported—for instance, in the case of the lauric acid phase-change nanocomposite with graphene nanoplatelet [83], carbon-based phase-change material [84], or magnesium chloride hexahydrate phase-change material composites [85]. Generally, it can be concluded that an increase in the concentration of nanomaterials dispersed in the phase-change materials increases the thermal conductivity. This may be misleading, since there is a limit to the amount of nanomaterial in the phase-change material—i.e., nanomaterials in larger fractions tend to agglomerate. Agglomeration may lead to a decrease or increase in thermal conductivity. It is hard to predict when agglomeration will occur since it depends on many parameters, such as the mass or volume fraction, size, and morphology of the nanomaterials, among others. Furthermore, the type, phase, and temperature of the phase-change material may also have a significant influence on this phenomenon.

Sharma et al. [86] prepared a nano-enhanced phase-change material composed of palmitic acid and nanoparticles of titanium oxide. The authors stated that the increase in the mass fraction of the nanoparticles causes the nano-enhanced phase-change material thermal conductivity to increase. A maximum increase in thermal conductivity of about 80% was recorded for 5% wt. loading of nanoparticles. For the same concentration of nanoparticles, there was a 15.5% decrease in latent heat of fusion with respect to the pure phase-change material.

Mayilvelnathan and Arasu [87] reported on the thermal conductivity measured by the laser flash method of pure erythritol phase-change material, i.e., erythritol with 0.1%, 0.5%, and 1% of graphene nanoparticles before as well as after thermal-cycling periods. The thermal conductivity of pure erythritol was 0.733 W/mK, whereas, when considering the erythritol with 0.1% wt., 0.5% wt., and 1% wt. of graphene nanoparticles, the thermal conductivity increased to 1.074, 1.095, and 1.122 W/mK. The thermal conductivity was 0.692, 0.899, 0.921, and 1.020 W/mK for pure erythritol without and with 0.1% wt., 0.5% wt., and 1% wt. of graphene nanoparticles, respectively. Additionally, the authors Putra et al. [88] studied the thermophysical characteristics of nano-enhanced phase-change materials based on Rubitherm paraffin wax, RT22 HC, and graphene nanoplatelets. The thermal conductivity of the phase-change material was increased by around 90% with the addition of 0.3% wt. of graphene.

Nourani et al. [89] modified paraffin with different mass fractions of alumina nanoparticles. The authors in the article claim that the character of the relationship between the effective thermal conductivity and increasing the alumina mass fraction was nonlinear for both the solid and the liquid phase. The enhancement ratio of the effective thermal conductivity was 31% in the solid phase and 13% in the liquid phase for the nano-enhanced phase-change material at 10% wt. of alumina. A reduction of 27% of the heating and

melting times was also detected for the same concentration of nanoparticles in the phase-change material.

Wang et al. [90] produced a stable OP10E and water emulsion enhanced by the inclusion of graphite nanoparticles. The authors argued that the supercooling effect of the emulsion could be prevented by the addition of graphite nanoparticles with a concentration superior to 2% wt. Furthermore, it was stated that the addition of graphite nanoparticles to the OP10E/water emulsion did not affect the latent heat. In the same study, it was found that 2% wt. of graphite nanoparticles resulted in a thermal conductivity increase of 88.9%.

4.2. Specific Heat

The specific heat of nanofluids depends primarily on the type, morphology, and concentration of the incorporated nanoparticles in the base fluid. Considering water as a base fluid, the published studies confirmed a considerable reduction in the specific heat of the water-based nanofluids, with the fundamental influencing factor for that to happen being the concentration of the nanoparticles added to the water. In this scope, the authors Zhou and Ni [91] prepared an aqueous alumina nanofluid at different concentrations ranging from 1.4% vol. to 21.7% vol. The differential scanning calorimetry technique was used to measure the specific heat of the nanofluids in a temperature range of between 20 °C and 45 °C. The research team observed decreases in the specific heat capacity of between 6% and 45% at concentrations of 1.4% vol. and 21.7% vol., respectively. Several other studies have investigated aqueous nanofluids with silica particles with dimensions of 32 nm [92] and 20 nm [93] and copper oxide particles with dimensions of 30 nm [94] and 23–37 nm [95] at various particle concentrations. These studies reported large decreases in the specific heat value with increasing nanoparticle concentrations. These lower specific heat values could have been a result of agglomerated nanoparticles in these samples, but a comprehensive characterization was reported. Like water-based nanofluids, ethylene glycol and ethylene glycol–water nanofluids showed decreases in specific heat from the values of pristine fluid. Although ethylene glycol had a lower specific heat value than water, it was still much higher than that of the particle materials. Thus, the proper trend of decreasing specific heat at higher particle concentrations was upheld in these studies. Additionally, the researchers Teng et al. [96] evaluated the specific heat of multi-walled carbon nanotubes dispersed in a mixture of ethylene glycol and water nanofluid at concentrations of 0.1% wt., 0.2% wt., and 0.4 wt.%, employing chitosan as a surfactant. The authors found that the inclusion of the multi-walled carbon nanotubes reduced the specific heat capacity of the base fluid mixture by between 2% and 8%, with the highest reduction shown by the most concentrated nanofluid. Furthermore, the researchers De Robertis et al. [97] analyzed the specific heat of a copper–ethylene glycol nanofluid at a 0.5% wt. of nanoparticles and at two different pH values. The pH of the primary nanofluid was 2.2, and a solution of sodium hydroxide was used to increase the pH to 10. The specific heat measurement revealed a decrease in specific heat in the nanofluids compared to the ethylene glycol-based fluid. The experiments showed a decrease of around 4% for the copper–ethylene glycol with the pH adjusted to 2.2 and a 12% decrease when the pH was adjusted to 10. It is likely that an increase in the pH moved the solution around the isoelectric point, perhaps resulting in an agglomeration of the nanoparticles in this case. From these available studies, it can be concluded that water and ethylene glycol nanofluids exhibit a decrease in specific heat with an increase in particle concentration and an increase in specific heat with an increase in temperature. In a more comprehensive pursuit of enhanced nanofluid-specific heat, a study by Starace et al. [98] explored various nanoparticle and base fluid combinations at different concentrations. The study used 36 different nanofluids with negligible changes in the heat capacity with respect to the base fluid. The authors used nanoparticles of silica, fumed silica, alumina needles, aluminum nitride, exfoliated graphite, iron core/iron oxide shell, bismuth, and mesoporous silica. The nanoparticles were dispersed in mineral oil, poly-α olefin, ethylene glycol, 60/40 by mass ethylene glycol/water, and calcium nitrate tetrahydrate. As some nanoparticles were suspended easily in some fluids and others required the use of

surfactants, the researchers defined specific mixing procedures for each combination. The results showed only small changes in the specific heat considering the overall scatter of measured specific heats over the temperature range investigated. It was suggested that a change in overall specific heat could be possible only if a rearrangement of the base fluid molecules to a higher heat capacity configuration was caused by the nanoparticles. Molecular dynamic simulations of copper nanoparticles in ethylene glycol [99] have shown an ordering layer of 0.75 nm thick around the nanoparticle; however, the specific heat of this predicted ordered layer has not been studied. Despite the high number of available experimental methods for evaluating the thermal transport of PCMs during the phase-change process, numerical simulations are also powerful tools for the optimized design of PCMs. Numeric simulations can accurately describe the phase-change heat transfer process by exploring diverse models like the energy balance method, finite element simulation, or commercially available computational fluid dynamics (CFD) software such as Ansys Fluent or COMSOL Multiphysics with Heat Transfer Module. The structural and operational parameters after optimization can provide guidance for the thermal enhancement of PCMs and thermal energy storage systems containing PCMs. As the most common analytical methods for solving engineering problems, the energy balance method and the enthalpy method are widely used to simulate the thermal transport behavior of PCMs during the solidification/melting stages. To simulate the thermal transport of PCMs in thermal energy storage systems more efficiently, the finite element method and the CFD modeling method are introduced, which can easily accomplish the simulation. The energy balance method is usually used to study the flow of energy based on energy conservation and to analyze the thermal enhancement effect in PCMs. The energy equation for a system without energy generation can be given by Equation (1):

$$E_{st} = E_{in} - E_{out} \tag{1}$$

where, in the cases of solar energy modules operating with PCMs, E_{st} is the energy transfer and energy retention between the different modules of the system, E_{in} is the received solar energy, and E_{out} is the energy loss of the system. When E_{st} of the PCMs needs to be considered, the energy equation between the PCMs and other parts should be used. Based on the flow and change in energy, the thermal enhancement effect can be reliably addressed and regulated, which further improves the thermal energy storage ability of PCMs. The enthalpy method is based on the enthalpy modifications of the different modules of a solar thermal energy system. The fundamental benefit of the enthalpy method is closely related to the capability of avoiding direct front tracking when dealing with materials that melt or solidify over a range of temperatures, which enable numeric simulation using complex geometries. The enthalpy equation for the solidification and melting processes can be expressed by Equation (2):

$$\frac{\partial(\rho H)}{\partial \tau} + \nabla \cdot (\rho v H) = \nabla \cdot (k \nabla T) + S \tag{2}$$

where H is the total enthalpy, ρ is the density of the operating fluid, v is the velocity of the operating fluid, and S is the source term defined by the condition of the sample. The total enthalpy can be determined by Equation (3):

$$H = h + \Delta H \tag{3}$$

where h is the sensible heat enthalpy and ΔH is the latent heat enthalpy. The sensible heat enthalpy is expressed by Equation (4):

$$h = h_{ref} + \int_{T_{ref}}^{T} C_p dT \tag{4}$$

where C_p is the specific heat capacity of the operating fluid and H_{ref} and T_{ref} are reference values. The initial condition $T_i = T(x,y,z,\tau_0)$ and boundary conditions like $k \cdot \partial T / \partial n = q_0$ and $-k \cdot \partial T / \partial n = h_s (T - T_o)$ should be used in the numeric simulation, where q_0 is the heat flux, h_s is the air surface heat transfer coefficient, and T_o is the ambient temperature. The governing equation of the enthalpy method is similar to the single-phase equation, providing an easier solution to the phase-change problems. Also, in the enthalpy method, there are no conditions to be satisfied at the solid–liquid interface, and this method yields a solution involving both solid and liquid phases [100]. For example, the researchers Han et al. studied the thermal energy storage and release processes in multi-cavity-microstructured PCM microcapsules and found that the charge and discharge velocity of PCMs were accelerated by increasing the number of cavities and cavity interlayers in the microcapsules [101]. The feature is that the enthalpy method possesses great suitability to be applied in the field of engineering thermal energy storage systems, providing a reliable evaluation for engineering applications of PCMs. The finite element simulation method subdivides a large phase-change energy storage system into smaller and simpler elements and simulates them separately, which is called the discretization strategy. There are many types of discretization strategies, such as the h-version and the p-version. Both of these versions are numerical methods for solving partial differential equations. Their main difference is that the polynomial degrees of the elements are fixed and the mesh is refined in the h-version, whereas the finite element mesh is fixed and the polynomial degrees of elements are enhanced in the p-version [102]. After the simulation, the subdivided elements are then assembled into a larger system, which makes it easier to model the thermal transport problem during the phase-change process. The finite element simulation method offers many options for regulating the complexity of both modeling and analysis in a heat transfer system. At the same time, it can also balance the necessary accuracy and computational processing time that can assess many of the concerns associated with engineering applications. The thermal performance of PCMs, as one of the most studied research topics in the technological field, can be reliably described via finite element simulations [103]. For instance, the researchers Wang et al. [104] studied the impact of the porosity and thermal conductivity of a metal foam on the thermal conductivity and melting of PCMs. The optimum fin structure was attained, which considerably increased the rate of solidification of the PCMs, opposite to the velocity increase via the action of the dispersed copper nanoparticles studied by the authors Lohrasbi et al. [105]. The finite element simulation method provides accurate prediction of the thermal enhancement effect for micro-/nano-PCMs. To achieve a highly efficient finite element simulation, CFD modeling was developed to analyze engineering situations with inherent complex problems, such as the solidification and melting processes in PCMs for solar thermal purposes. This method also involves fluid mechanics such as turbulence models and two-phase flow, which focus on the flow of gas and liquid and can resolve the intricate restriction of the fluid flows in solar thermal research and technology, like the flow of heat transfer fluids at various flow rates. Therefore, to analyze the thermal enhancement during the solidification process of PCMs or the heat exchange process of colloidal suspensions, CFD is undoubtedly an ideal numerical simulation method. Moreover, the researchers Mahdi et al. [106] combined nanoparticles with metal foam or metal fins in a thermal energy storage system containing triplex-tube PCMs and confirmed the thermal enhancement provoked by this solution for the improvement of the thermal energy storage system. Further work on PCM thermal energy storage analysis will undoubtedly require the development of CFD modeling with enhanced computing processing capacity. Also, to seize the internal and external thermal energy exchange of PCMs or PCMs operating in thermal energy storage systems, the combined exploration of experimental findings and numeric simulations is a vital tendency that should be maintained. For thermal conductivity and the drastic augmentation of the latent heat of PCMs or the use of the thermal energy in a thermal energy storage system, this combination provides accurate data and reliable evidence for the optimized design of thermal energy storage systems using PCMs. Figure 8

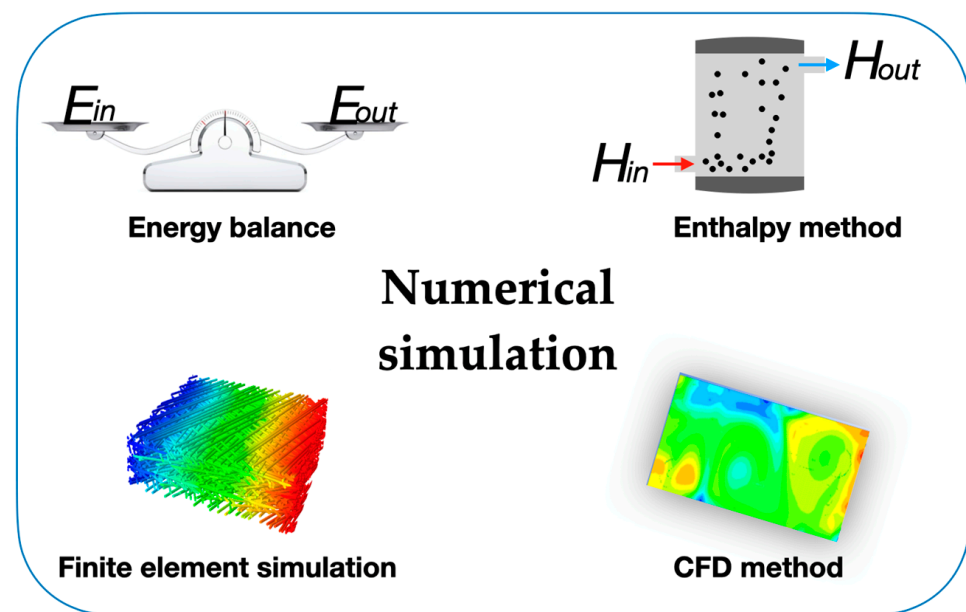summarizes the fundamental formulations for the numerical simulations involving PCMs and nano-enhanced PCMs.

Figure 8. Main formulations for numerical simulations involving PCMs.

Moreover, the authors Starace et al. [98] also referred to many experimental works investigating the ordered layer of the water around proteins and hydrophobic molecules, where the water molecules are almost immobile in that layer, providing an increase in the specific heat of the system proportional to the volume of the ordered layer interface. Hence, the authors concluded that, to have an increase in the specific heat of nanofluids, the layered structure should have a specific heat many times higher than that of the base fluid. This ordered interfacial structure will be discussed in more detail in the next section. Furthermore, the authors Shin and Banerjee [107] and Tiznobaik and Shin [108] investigated the binary eutectic salt Li_2CO_3-K_2CO_3 (62:38) with the addition of 1% wt. of silica nanoparticles in different sizes. Their experimental works reported enhancements of around 25% in the specific heat regardless of the size of the nanoparticles. In addition, the obtained TEM images of the nano-enhanced salts after a melting and freezing process showed the formation of needle-like nanostructures in the salt, which could be the main reason behind the improved specific heat. Nonetheless, these special nanostructures within the molten salt were not observed in other published studies. Moreover, the researchers Dudda and Shin [109] investigated the binary eutectic salt $NaNO_3$-KNO_3 (60:40), commonly designated as solar salt given its suitability for commercial solar thermal power plants as a thermal energy storage medium, with the incorporation of silica nanoparticles. In their first study, the authors added 1% wt. of silica nanoparticles in two different sizes and confirmed a 19% enhancement in the specific heat for the 5 nm nanoparticles and a 25% increase when adding 30 nm nanoparticles. In their subsequent experimental work [110], the researchers added the same fraction of silica nanoparticles and found enhancements in the specific heat of 8%, 12%, 19%, and 27% with nanoparticles in sizes of 5 nm, 10 nm, 30 nm, and 60 nm, respectively. Furthermore, the authors Lu and Huang [111] evaluated the specific heat of molten $NaNO_3$-KNO_3 (60:40) salt containing alumina nanoparticles 9 nm and 13 nm in size. The concentrations used were superior to 1% wt., and a decrease in the specific heat capacity of the nanofluid was found. Also, it was verified by the authors that the specific heat decreased with increasing concentration and size of the nanoparticles. Additionally, the researchers Chieruzzi et al. [112] studied $NaNO_3$-KNO_3 (60:40) salt with the addition of alumina nanoparticles at concentrations of between 0.5% wt. and 1.5% wt. and reported an increase in the specific heat of 5.9% at 1% wt. and decreases in the specific heat at 0.5% wt.

and 1.5% wt. Also, the researchers Ho and Pan [113] confirmed a nearly 20% enhancement in the specific heat at a very reduced concentration of 0.063% wt. of alumina nanoparticles in the ternary eutectic salt KNO_3-$NaNO_2$-$NaNO_3$. Interestingly, increases in temperature were shown to decrease the specific heat of the salt, which is not in agreement with any other study, all of which showed constant or increasing specific heat with temperature. The specific heat enhancement of the molten salts with the addition of nanoparticles was attributed by the authors Shin and Banerjee [114,115] to three different possible mechanisms. The first one is related to the higher specific heat capacities of nanoparticles themselves, which is possible when the size of the particles is decreased. At present, nanoparticle-specific heat values have only been investigated up to 350 K [116], indicating that their properties at the high operating temperatures of molten salts is still largely unknown—a topic that should be investigated further. Also, the authors suggested that a high surface area per unit mass of nanoparticles increases the interfacial thermal resistance between nanoparticles and the surrounding liquid molecules. This high interfacial thermal resistance acts as additional thermal storage due to the interfacial interaction of the vibration energies between nanoparticle atoms and the interfacial molecules. This phenomenon could cause an increase in the specific heat of the salts [115]. Finally, the semi-solid behavior of layered liquid molecules at the surface of solid particles must be considered. The semi-solid layer can be visualized as a liquid–solid phase change at the surface and has been shown to have higher thermal properties than the bulk liquid and be equivalent to a latent phase change heat. Also, the researchers Jung and Banerjee [117] carried out molecular dynamics simulations to investigate this mechanism and introduced an analytical model to determine the specific heat of the salts. The empirical model for this mechanism simply assumes values for the semi-solid layer thickness, which could vary for different salts and particle materials and sizes. Moreover, the authors Shin and Banerjee [115] estimated that the semi-solid layer of liquid molecules on a crystalline surface can reach 2–5 nm in thickness—with this range depending on the surface energy of the crystalline interface. Thus, the mass fraction of the semi-solid layer should increase proportionally with the reduction in the size of the nanoparticles (for the same concentration of nanoparticles). Consequently, smaller nanoparticles should cause a greater enhancement in the specific heat of nanofluids. However, constant enhancement with different sizes of nanoparticles [115] and more enhancements with larger particles [112] have been reported, which seems to contradict this part of the theory. It is possible, though, that these unexpected trends could be explained by clustering at high temperatures, resulting in different particle size distributions during testing. The ionic liquid-based solvation force stability, as previously described, is also based on the existence of layered structures of ions in the vicinity of the solid–liquid boundary. Therefore, the common concept of the ionic liquid interfacial structure and semi-solid layers indicate a plausible mechanism to produce a stable colloidal system with enhanced specific heat. However, this is unproven for molten salts and still requires further investigation. On the other hand, the nanocomposites had lower specific heat compared to the base PCM, such as, for example, in the case of the improvement in photo-thermal performance [90], for PCM-filled cylinders [88], and in thermoelectric applications [118]. On the contrary, the authors Chieruzzi et al. [119] found that nanocomposites had a higher specific heat than that of the corresponding base PCM. The researchers prepared a nanofluid based on a nitrate salt mixture of 60% wt. $NaNO_3$ and 40% wt. KNO_3, T_m 220 °C. To create the nano-enhanced PCM, silica (7 nm), alumina (13 nm), and a mixture of silica and alumina (2–200 nm) nanoparticles at 1% wt. were added to the nitrate salt mixtures. The best results were achieved for the nanofluid with 1% wt. of silica/alumina nanoparticles. The specific heat in the solid phase was improved by around 52 and in the liquid phase by around 19%. The stored heat was increased by 13.5% compared with that of the PCM itself. On the other hand, the researchers Liu and Yang [120] enhanced the thermal properties of inorganic hydrate salt with titanium oxide–P25 nanoparticles with a dimension of 21 nm. The specific heat was improved by 83.5% in the solid phase and by 15.1% in the liquid

phase by adding 0.3% wt. of nanoparticles. Furthermore, the latent heat was increased by 6.4%.

4.3. Latent Heat

In most studies, the addition of nanomaterials caused a slight decrease in the latent heat, except in [119] in relation to the passive cooling application and in [120] for the case of hydrate salts, where increases of 10.8% and 6.4% were reported, respectively, whereas in [121], the addition of graphite nanoparticles to an OP10E/water emulsion did not affect the latent heat. Also, the authors Warzoha et al. [122] found that the latent heat of fusion of organic paraffin decreased with the percentage of herringbone graphite nanofibers. The latent heat of fusion of the pure paraffin PCM was 271.6 J/g, whereas the latent heat of fusion of the nano-enhanced PCM with 11.4 vol% of graphite nanofibers was 242.7 J/g. The thermal conductivity and diffusivity increased with the increase in volume fraction of the HGNF. Furthermore, the authors Colla et al. [82] added alumina and carbon black nanoparticles to the paraffin waxes RUBITHERM®RT20 and RUBITHERM®RT25. The authors claimed that the addition of 1% wt. of alumina nanoparticles caused a degradation in thermal conductivity in both PCMs by 7–8%, whereas 1% wt. of carbon black nanoparticles increased the thermal conductivity by more than 25%. When alumina nanoparticles were added to RT20, the improvement in the latent heat was 10.8%, whereas in the case of carbon black nanoparticles the improvement was only 3.4%. The addition of carbon black nanoparticles to RT25 caused a reduction in latent heat of 11.6%. Moreover, the authors Muthoka et al. [123] prepared barium chloride dehydrate solutions in which nanoparticles of magnesium oxide and multi-walled carbon nanotubes were added. The authors stated that a 7% reduction in latent heat was detected for 1% wt. of multi-walled carbon nanotube0-enhanced fluid and a 5.2% reduction for 1% wt. magnesium oxide-enhanced fluid. Furthermore, the researchers Ebadi et al. [118] enhanced coconut oil with nanoparticles of copper oxide to create biobased nano-enhanced PCMs. A nanocomposite with 1% wt. of nanoparticles had 7.5% higher thermal conductivity than the base PCM, whereas the specific heat and latent heat of fusion decreased by 0.75% and 8.2%, respectively.

In Section 3, the literature results related to the most relevant thermophysical properties of nanofluids were presented, and several discrepancies were discussed. Regarding thermal conductivity, such divergences may have arisen from the techniques used to measure this property, as exemplified in Figure 5 of this paper. Many of these techniques are adaptations of methods traditionally used to measure solids, powders, and gases, as mentioned in [124]. Another factor to be considered concerns the methodology used by researchers in the literature; the possibilities for preparing nanofluids can vary considerably between different studies, as seen in Figure 3. Even in two independent studies that use the same nanofluids, with identical concentrations and particle diameters, the lack of a common protocol that considers the pH, the dispersion technique adopted, whether surfactants were used, and the type of base fluid can influence the measurements of the thermal properties.

5. Main Solar Thermal Conversion and Harvesting Applications

5.1. Solar Thermal Energy Storage Systems

Most nano-enhanced PCMs are very suitable for the thermal energy storage technological field. Thermal energy storage systems based on a nano-enhanced PCM operate according to the passive energy storage principle of latent heat. Such systems allow an active thermal management of the release and storage of latent heat. The main limiting parameter is the phase-change temperature value or temperature value range. Also, the choice of the most suitable nano-enhanced PCM and nanofluid for a given system should be based on the ease of the preparation method and the cost, as well as on their improved thermophysical properties. The fundamental interest of researchers was directed towards the amelioration of the thermal conductivity of nano-enhanced PCMs. The authors Lin and Al-Kayiem [125] conducted an experimental study on the thermophysical properties of nano-enhanced PCMs used in a solar collector. The experimental results demonstrated

that the addition of 1% wt. of copper nanoparticles to the base paraffin wax increased the solar collector efficiency by 1.7% compared to that attained with a pure PCM. Also, the authors Natividade et al. [3] studied the thermal efficiency of a solar collector system with a parabolic concentrator. In their experiments, a nanofluid composed of water and multilayer graphene at extremely low volume fractions of 0.00045% vol. and 0.00068% vol. to prevent agglomeration and sedimentation was used. Despite having only a shallow description of the preparation method, with no references about the synthesis parameters or the equipment used, the nanofluid at 0.00045% vol. increased the thermal efficiency by 31% and the nanofluid at 0.00068% increased the same parameter by 76% compared to the results obtained with the water-based fluid alone. Additionally, the researchers Altohamy et al. [16] studied the inclusion of an aqueous alumina nanofluid in a latent heat thermal energy storage system. The authors confirmed that the use of the nanofluid had an impact on the solidified mass fraction and charging time of the system, which decreased considerably. Moreover, the authors found appreciable improvements in the charging rate and amount of energy stored. The charging time was reduced by up to 30% at a volume fraction of 2% vol. compared to that achieved with pure water. Additionally, the authors Kannan and Nadaraj [126] improved the efficiency of a solar flat-plate collector simultaneously employing nanofluids and PCMs. The researchers used the solar water heater during the off-shine hours using a PCM, which maintained the heat even after the sunshine was gone. Therefore, during off-sunshine hours, it yielded a better thermal performance. The performance of the solar collector could be improved by increasing the absorber plate area and the size of the water tubes. The performance of the solar water heater with a PCM was improved by selecting an appropriate PCM with a high thermal storage capacity. It was also improved by increasing the quantity of the PCM and heat transfer area by fixing the absorber with better performance. By using an alumina nanofluid as a heat transfer fluid at a concentration of 0.01% wt., the instantaneous efficiency of the collector was enhanced from 0.9% to 3.4% and from 0.1 to 3.5 under mass flow rates of 20 L per h and 40 L per h. The thermal efficiency of the collector was increased from 1% to 2.9% and from 0.05 to 1.9 under the same mass flow rates. Figure 9 shows the schematic representation of the adopted photovoltaic/thermal system configuration.
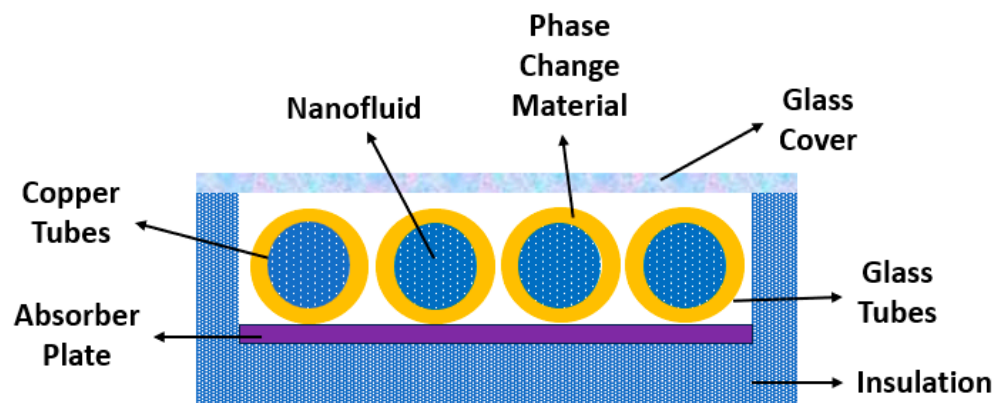

Figure 9. Configuration of the photovoltaic/thermal system. Adapted from [126].

5.2. Photovoltaic/Thermal Systems

The incoming solar radiation on the surface of the photovoltaic/thermal equipment may produce a large amount of electric power. Nonetheless, the absorbed solar radiation increases the temperature of the photovoltaic module and, consequently, decreases its overall efficiency. It is often stated in the published literature in the field that an increment in the temperature of photovoltaic panels causes an efficiency reduction of nearly 0.5% per degree [127], depending on the explored photovoltaic technology. Figure 10 schematically represents a typical photovoltaic/thermal system.
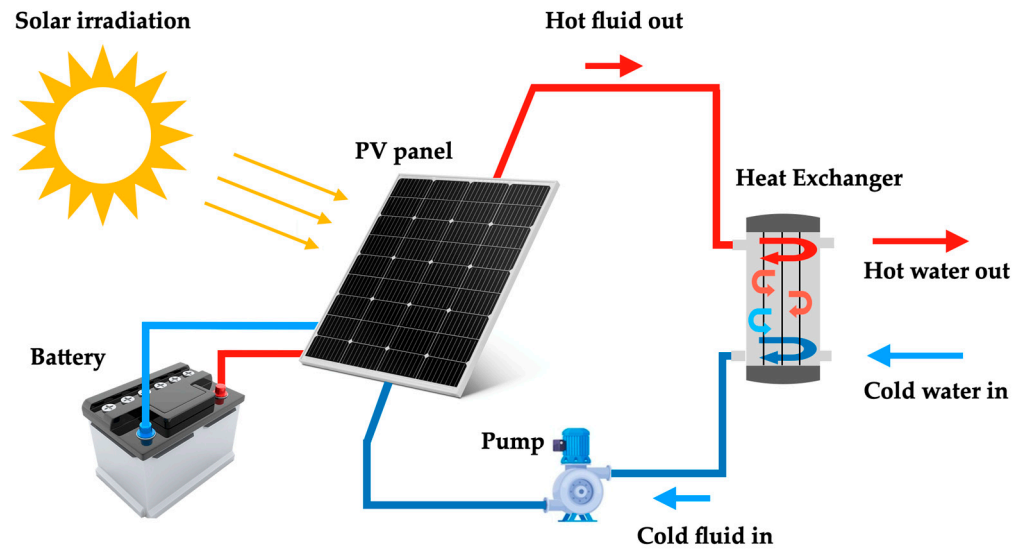
Figure 10. Schematic representation of a typical photovoltaic/thermal system.

Figure 11 schematically represents the energy and exergy associated with the control volume of a photovoltaic/thermal system.
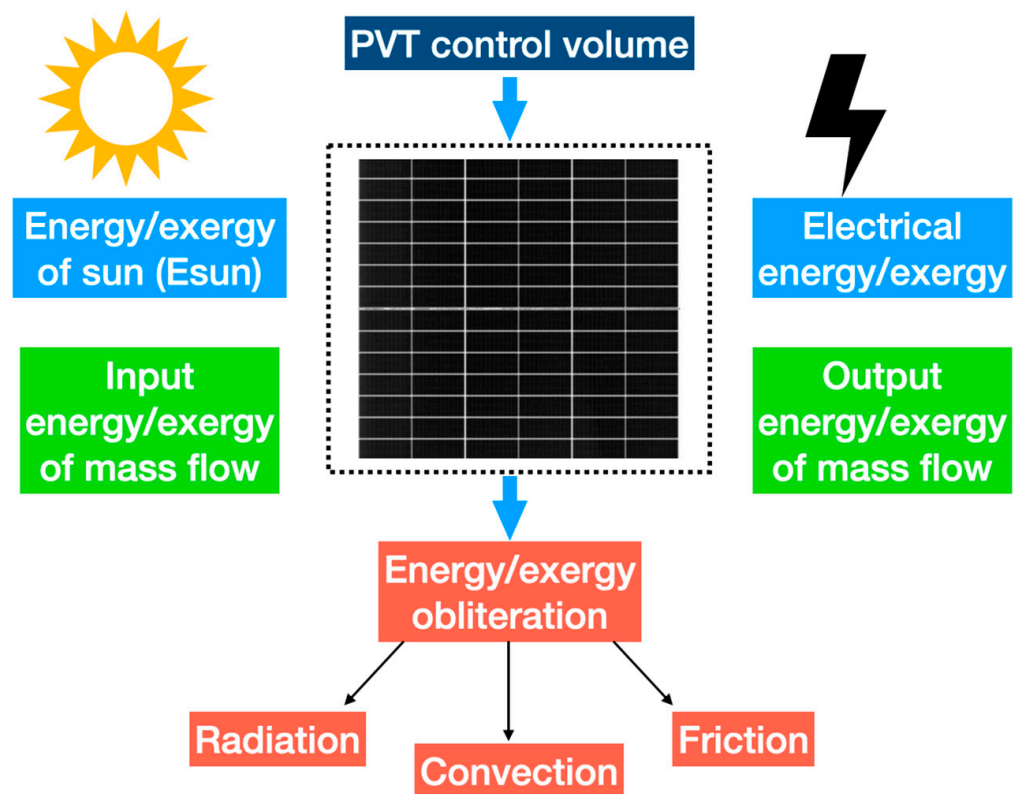

Figure 11. Energy and exergy of the control volume of a photovoltaic/thermal system.

The overall performance of a photovoltaic/thermal system can be evaluated based on a thermodynamic approach from the viewpoint of the first and second laws. The first and second laws may be referred to as energy and exergy analyses, respectively. Whereas an energetic analysis determines the quantity of the energy, an exergetic analysis determines its quality. Hence, considering the photovoltaic module and the thermal collector as a single control volume, the input energy is the quantity of solar irradiation and the output

energies are the electrical and thermal ones. Assuming a steady-state condition, the control volume energy balance can be given by Equation (5):

$$E_{in} = E_{el} + E_{th} - E_{loss} \tag{5}$$

where E_{in} is the incident solar irradiation to the photovoltaic/thermal system, E_{el} is the output electrical power, E_{th} is the thermal energy gained from the collector, and E_{loss} is the energy loss for the control volume. Moreover, the overall efficiency of a photovoltaic thermal system η_{PV} is the ratio of the output energies to the input energy during a defined period and is given by Equation (6) [128]:

$$\eta_{PV} = \frac{E_{th} + E_{el}}{E_{in}} = \frac{\int_{t_1}^{t_2} \left(A_c E_{th}^{'} + A_{pv} E_{el}^{'}\right) dt}{A_c \int_{t_1}^{t_2} G_{eff}^{'} dt} = \eta_{th} + r\eta_{el} \tag{6}$$

where A_c is the area of the collector, A_{pv} is the area of the photovoltaic cells, $E_{th}^{'}$ is the rate of output thermal energy per unit area of the collector, $E_{el}^{'}$ is the rate of output electrical energy per unit area of photovoltaic cells, G_{eff} is the rate of the effective incident radiation per unit area of the collector, η_{th} is the thermal efficiency of the system, η_{el} is the electrical efficiency of the system, and r is the packing factor given by the ratio A_{pv}/A_c. Furthermore, the term E_{th} can be determined by Equation (7):

$$E_{th} = m \cdot C_p \cdot (T_{fo} + T_{fi}) \tag{7}$$

where m is the mass flow rate through the collector of the operating fluid, C_p is the specific heat capacity of the operating fluid, T_{f0} is the outlet temperature of the fluid, and T_{fi} is the inlet temperature of the fluid. The electrical efficiency η_{th} can be expressed by Equation (8):

$$\eta_{el} = \frac{E_{el}}{E_{in}} = \frac{VOC \times ISC \times FF}{G_{eff}} \tag{8}$$

where VOC is the open-circuit voltage, ISC is the short-circuit current, and FF is the filled factor that defines the maximum power conversion efficiency of the photovoltaic module, which can be determined by Equation (9) [129]:

$$FF = \frac{P_m}{VOC \times ISC} \tag{9}$$

where P_m is the ideal output power. In Equation (8), $G_{eff}^{'}$ can be given by Equation (10):

$$G_{eff} = \tau_g \cdot \alpha_{cell} \cdot G \tag{10}$$

where τ_g is the glass surface transmissivity, α_{cell} is the cell absorptivity, and G is the rate of the incident irradiation. To infer the thermal energy of the photovoltaic/thermal systems, the output electrical energy should be converted into thermal energy using a conversion factor c_f. For most of the developed photovoltaic/thermal fluid systems, C_f values of 0.35 to 0.40 have been proposed [130]. Therefore, the overall equivalent photovoltaic/thermal system can be given by Equation (11):

$$\eta_{PV,TH} = \eta_{th} + r\frac{\eta_{el}}{C_f} \tag{11}$$

Similar to the energy analysis, by considering the photovoltaic module and the thermal collector as a unified control volume, the exergy balance can be expressed by Equation (12):

$$Ex_{in} = Ex_{el} + Ex_{th} - Ex_{loss} \tag{12}$$

The terms in Equation (12) are defined similarly to the terms of the energy balance, but in an exergy expression. In addition, the overall exergetic efficiency of the photovoltaic/thermal system can be given by Equation (13) [128]:

$$\varepsilon_{pv} = \frac{Ex_{th} + Ex_{el}}{Ex_{in}} = \frac{\int_{t_1}^{t_2} \left(A_c Ex'_{th} + A_{PV} Ex'_{el}\right) dt}{A_c \int_{t_1}^{t_2} Ex'_{sun} dt} = \varepsilon_{th} + r\varepsilon_{el} \tag{13}$$

where ε_{pv} is the overall exergetic efficiency, ε_{th} is the thermal exergetic efficiency, ε_{el} is the electrical exergetic efficiency, Ex'_{th} is the rate of output thermal exergy per unit area of the collector, Ex'_{el} is the rate of output electrical exergy per unit area of the cells, and Ex'_{sun} is the rate of the incident irradiation exergy per unit area of the collector. In the equation above, the thermal and electrical output exergies can be linked with the output energies by Equations (14) and (15), respectively:

$$Ex_{el} = E_{el} \tag{14}$$

$$Ex_{th} = E_{th} \cdot \left(1 - \frac{T_a}{T_{fo}}\right) \tag{15}$$

where the temperatures are expressed in Kelvin and T_a is the ambient temperature. The received input exergy can be determined by Equation (16) [131]:

$$Ex_{sun} = G\left[1 - \frac{4}{3}\frac{T_a}{T_{sun}}(1 - \cos\beta)^{\frac{1}{4}} + \frac{1}{3}\left(\frac{T_a}{T_{sun}}\right)^4\right] \tag{16}$$

where T_{sun} is the equivalent temperature of the sun as a blackbody of nearly 5800 K and β is the half-angle of the cone subtended by the sun disc, where β is around 0.0047 radian on a clear day for a beam sunlight and around $\pi/2$ radian for diffuse sunlight [132]. Figure 12 summarizes the fundamental thermal mechanisms associated with a photovoltaic/thermal system. The temperature at which a photovoltaic module operates is at equilibrium between the heat generated by the photovoltaic module and the heat loss to the surrounding environment. The various thermal processes of heat loss are reflection, radiation, convection, and conduction. The conductive heat loss is derived from the different temperatures between the photovoltaic module and the other materials with which the photovoltaic module is in contact. The capability of the photovoltaic module to transport heat to its surroundings can be symbolized by thermal resistance. The convective heat transfer arises from the transport of heat away from a surface as the result of one material moving across the surface of another. In a photovoltaic module, the forced convective heat transfer is generated by the wind blowing across the surface of the cell. The free or natural convection exchange of the panel with the area surrounding it has a smaller impact. This natural convection is caused by the air temperature and can be defined by Newton's law of cooling. The free convection becomes considerable in cases where only a little wind blows under cold climates, in which the temperature gradient between the surface of the photovoltaic module and the ambient air is relatively large. Also, the photovoltaic module may transfer heat to the surrounding environment through reflection and radiation. In the exchange of heat via radiation, long-wave radiation may be involved. To determine its contribution to the heat balance, it is necessary to consider the value of the radiative conductance or emissivity between the surfaces of both sides of the photovoltaic panel with both the ground and the sky.

Hence, considering the efficiency and economic feasibility of photovoltaic/thermal systems, it is reasonable to consider that their innovative thermal regulation and the beneficial thermophysical characteristics of nano-enhanced PCMs may be very suitable for this end. In recent years, many different new photovoltaic/thermal technologies have emerged other than those of air, water, and employing two thermal fluids with some desirable output. The heat transfer capability depends on the thermal conductivity of

the cooling media. Dispersing highly conductive nanoparticles into the cooling fluid improves the thermal conductivity of the cooling medium, and the heat transfer rate is also increased. Figure 13 summarizes the fundamental design of and operating parameters for a photovoltaic/thermal system to operate with nanofluids and PCMs.
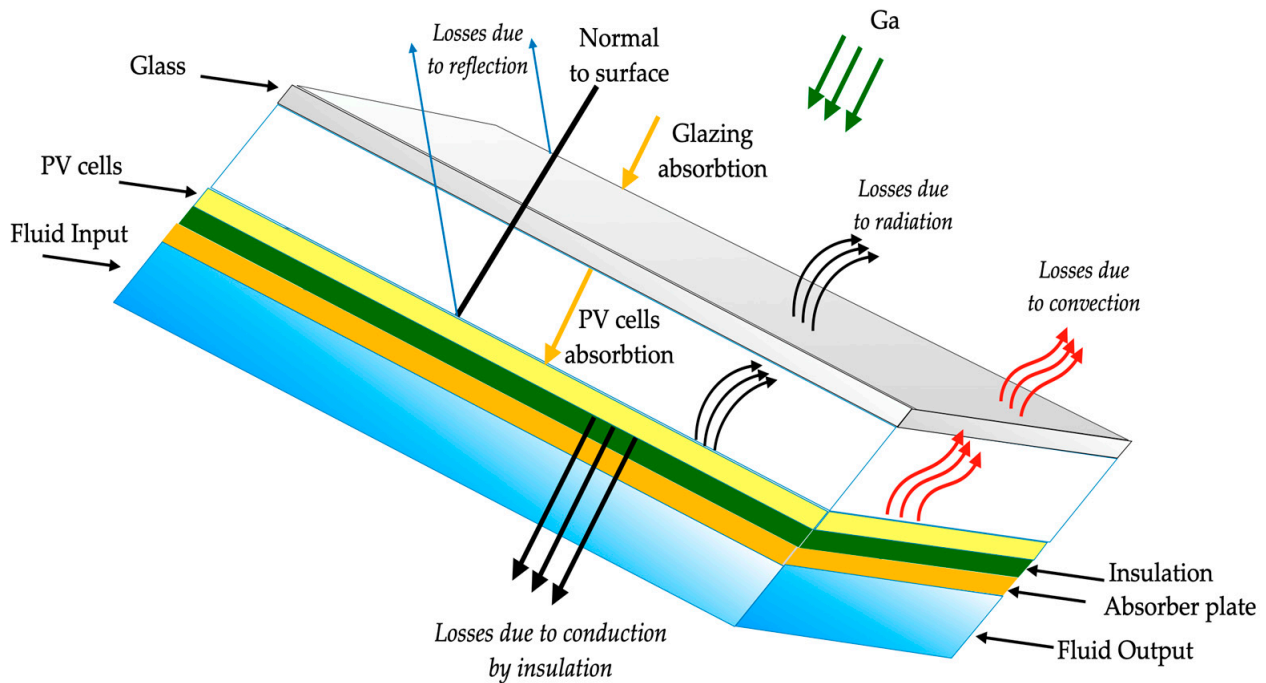

Figure 12. Main heat transfer mechanisms associated with a photovoltaic/thermal system.
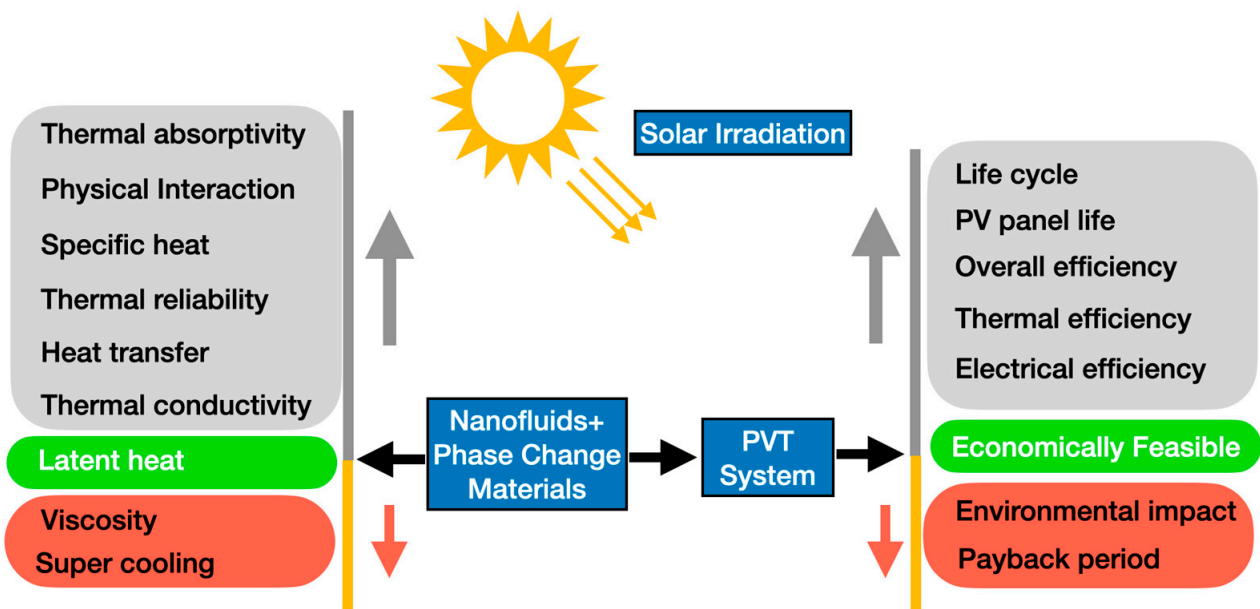

Figure 13. Main design parameters for a photovoltaic/thermal system operating with nanofluids and PCMs.

Table 1 summarizes the benefits and disadvantages of the different cooling media in photovoltaic/thermal systems.

Table 1. Main benefits and disadvantages of the different cooling media in photovoltaic/thermal systems.

Photovoltaic/Thermal System	Cooling Medium	Benefits	Problems	Applications
PCM-integrated photovoltaic/thermal system	Air	Low investment cost Easy to install and maintain Less bulky system Air availability	Poor thermal conductivity Low heat transfer capability Low photovoltaic panel temperature reduction Low thermal performance Fan is required for circulating the air Some of the PCMs may leak during melting	HVAC Residential buildings Thermal space management
PCM-integrated photovoltaic/thermal system	Water	Higher heat transfer capability than the one with air as a coolant Suitable for different fluidic coolants	High investment cost Low thermal conductivity High maintenance cost Risk of equipment corrosion Freezing Leakage High power consumption	HVAC Residential buildings Thermal space management
PCM-integrated photovoltaic/thermal system	Nanofluid	Advanced technology Enhanced heat transfer capability Broad range of commercially available nanoparticles	High pumping power is required Stability of the dispersion of nanoparticles in the base fluid High cost of nanoparticles Leakage and fouling risks	HVAC Residential buildings Thermal space management
Nano-enhanced PCM-integrated photovoltaic/thermal system	Air	Advanced technology	Fan or blower is required Only average thermal performance	HVAC Water heating Snow and ice removal All-season thermal comfort Clothing washing and drying
Nano-enhanced phase-change material-integrated photovoltaic/thermal system	Water	Well -developed technologySuitable for different fluidic coolants Enhanced heat transfer capability	Settling of nanoparticles after several operating cycles Leakage	HVAC Water heating Snow and ice removal All-season thermal comfort Clothing washing and drying
Nano-enhanced phase-change material-integrated photovoltaic/thermal system	Nanofluid	Well-developed technology Very high thermal performance Broad range of commercially available nanoparticles	High pumping power is required Stability over time of the dispersion of the nanoparticles in the PCM and base fluid Settling of nanoparticles	HVAC Water heating Snow and ice removal All-season thermal comfort Clothing washing and drying

In this direction, the authors Nada and El-Nagar [133] evaluated the efficiency of PCMs and nano-enhanced PCMs in the thermal management of integrated photovoltaic modules. In view of the obtained results, it was found that, for the integrated modules, the inclusion of a PCM composed of paraffin wax and Rubitherm® RT55 and a nano-enhanced PCM with the addition of 2% vol. of alumina nanoparticles resulted in an increase in the photovoltaic efficiency of the system. The researchers reported that the daily efficiency was increased from nearly 5.7% using the PCM and from around 13.1% employing the nano-enhanced PCMs. Moreover, the researchers Al-Waeli et al. [134] added silicon carbide nanoparticles with concentrations of up to 4% wt. to a paraffin PCM to determine the thermal and electrical performance of a hybrid photovoltaic/thermal panel. The authors found that the heat dissipation from the photovoltaic/thermal panel was more uniform when the PCM was incorporated. Also, the PCM enhanced the efficiency of the system from 7.1% to 13.7% in comparison to common photovoltaic systems. Furthermore, the combined effect of aqueous zinc oxide nanofluids and a paraffin wax PCM was experimentally investigated by the authors Sardarabadi et al. [135] in a photovoltaic/thermal system. The concentration of the nanofluids varied from 0.1% wt. and 0.4% wt. and the researchers observed that the electrical efficiency of the system was increased by 13%. The efficiency of the photovoltaic/thermal system incorporating the nanofluids was 5% higher than the one with water. Also, the paraffin wax further improved the efficiency of the photovoltaic panel by 9%. Figure 14 schematically illustrates a typical configuration of the combined use of nanofluids and PCMs in a photovoltaic/thermal system.
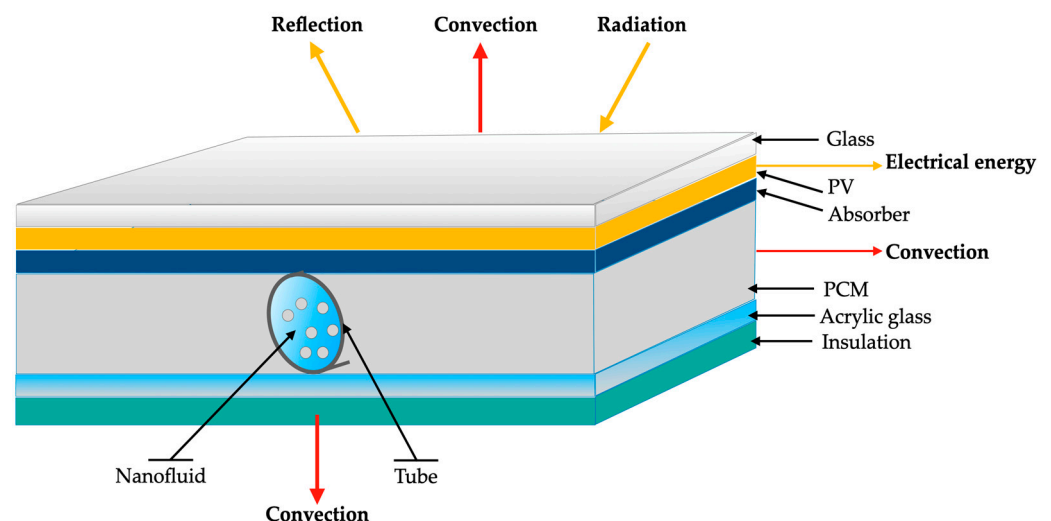

Figure 14. Typical configuration of a photovoltaic thermal system operating simultaneously with nanofluids and PCMs.

Additionally, the authors Hosseinzadeh et al. [136] evaluated the energy and exergy efficiency of a photovoltaic module, a photovoltaic/thermal system using a nanofluid, and a photovoltaic/thermal system operating with a nanofluid and a PCM. A zinc oxide–water nanofluid and a paraffin PCM were used. The obtained results indicated that the electrical efficiencies of the photovoltaic module, the nanofluid photovoltaic/thermal system, and the nanofluid and PCM photovoltaic/thermal system were around 12.6%, 13.4%, and 14.1%, respectively. The overall efficiencies were approximately 12.6%, 53.3%, and 65.7%, respectively. The thermal efficiencies of the nanofluid photovoltaic/thermal system and the nanofluid and PCM photovoltaic/thermal system were around 39.9% and 51.7%, respectively. Also, the exergy efficiencies of the possible alternatives were about 10.7%, 13.6%, and 12.4%, respectively. In addition, the nanofluid and PCM photovoltaic/thermal equipment provided an increase of 26% in the thermal efficiency in comparison to that attained with the conventional system. Moreover, the researchers Sardarabadi et al. [135] evaluated the performance of a PCM photovoltaic/thermal system operating according

to distinct configurations and with diverse heat transfer fluids. A conventional water operating system, a zinc oxide aqueous nanofluid operating system, a water- and PCM-integrated system, and, finally, a zinc oxide nanofluid- and PCM-integrated system were studied. The obtained results indicated that this last approach exhibited the greatest overall thermal and electrical efficiencies and the most reduced photovoltaic panel surface temperature. The research team concluded that the nanofluid–PCM-integrated system provided increased electrical and overall efficiencies of 13% and 23%, respectively, with respect to those achieved with a conventional photovoltaic system without requiring any extra consumption of energy. This system also yielded a 48% increase in thermal energy in comparison with the one provided by the nanofluid operating system. Also, the temperature reduction of the photovoltaic panel was of only 10 °C when the system operated with water cooling, whereas the use of the nanofluid–PCM-integrated system reduced the homologous temperature by 16 °C. Figure 15 schematically presents the general view of the experimental setup developed by the authors.
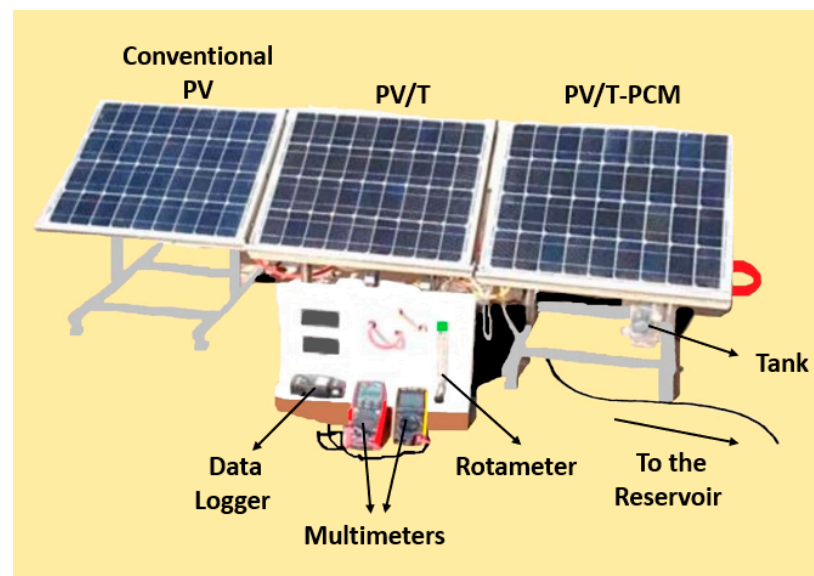

Figure 15. General view of the experimental setup developed by the authors Sardarabadi et al. Adapted from [135].

Moreover, the authors Hassan et al. [137] investigated the performance of a photovoltaic/thermal system using a PCM and nanofluids simultaneously. Flow rates of between 20 and 40 L per min and volumetric concentrations of nanofluids of 0.05% vol. to 0.15% vol. were imposed. A conventional photovoltaic system, a PCM operating system, a water- and PCM-integrated operating system, and a nanofluid- and PCM-integrated operating system were examined. The investigation team concluded that the nanofluid–PCM-integrated system achieved the best performance at 0.1% vol. and with a flow rate of 40 L per minute. This system attained electrical energy, thermal energy, and overall performances of 14%, 45.8%, and 60.3%, respectively.

The researchers Al-Waeli et al. [134] developed nanofluid nano-enhanced PCM photovoltaic/thermal equipment with an imposed flow rate of 0.17 kg/s. The authors verified that there was a considerable decrease in the temperature of the surface of the photovoltaic panel. The temperature of the photovoltaic panel was reduced by up to 30 °C during the peak solar irradiation time. Also, the obtained results showed that the open-circuit voltage, power, and electrical efficiency increased from 13 V to 21 V, from 61.1 W to 120.7 W, and from 7.1% to 13.7%, respectively. The researchers also reported a 72% increase in the thermal efficiency of the device. Furthermore, the researchers Al-Waeli et al. [138] evaluated various cooling methodologies for a photovoltaic/thermal system using experimental data and artificial neural network software. The results confirmed that the integrated

nano-enhanced PCM–nanofluid approach exhibited superior performance with respect to the other photovoltaic/thermal systems. Additionally, the integrated nanofluid–PCM system had superior performance, and the electrical current and electrical efficiency increased from 3.69 A to 4.04 A and from 8.07% to 13.2%, respectively, compared to the conventional photovoltaic systems. Also, the authors compared the experimental results with artificial neural network software and discovered that the neural model was in good agreement with the experimental results. On the other hand, the researchers Sarafraz et al. [139] analyzed the experimental and theoretical work of a photovoltaic/thermal PCM system. In their study, the authors analyzed the optimum pH value of the solution and flow rate of the cooling fluid to obtain a uniform dispersion and enhanced performance. The highest electrical and thermal performance was attained at 0.2% vol. of multi-walled carbon nanotubes for the nano-enhanced PCM and nanofluid. The results showed that the thermal and electrical performances were improved by 130% and 20%, respectively using the multi-walled carbon nanotubes dispersed in paraffin as a nano-enhanced PCM and multiwalled carbon nanotubes dispersed in WEG50 as nanofluids. The authors also found a considerable reduction in the temperature of the photovoltaic panel. Also, the equivalent electrical and thermal powers at the maximum time were 276.3 W/m^2 and 307.9 W/m^2, respectively.

The researchers Al-Waeli et al. [140] analyzed the enhancement of the power production performance of a photovoltaic/thermal device using an artificial neural network and a mathematical model with three different cooling methods. The authors proposed three linear models. The first model is to find the best parameters to predict the production of power. The second one is to obtain identities that are closer to experimental results, and it is represented by its speed, low cost, and ease of use. The third model is to speed up the reflection of the best conditions for any innovative system to be designed or developed. The developed model aids to minimize the errors of further studies and find the best conditions for the photovoltaic/thermal device to operate. Moreover, the researchers Al-Waeli et al. [141] studied an artificial neural network model and experimentally evaluated the photovoltaic/thermal device under the same environmental conditions. They examined a conventional photovoltaic system, a water photovoltaic/thermal system, a nanofluid operating photovoltaic/thermal system, and a nanofluid–PCM-integrated system. The investigation team noted that the nanofluid–PCM system yielded the best performance, with thermal and electrical efficiencies of 72% and 13.3%, respectively. Additionally, the artificial neural network model results were found to be consistent with the obtained experimental results and with those published earlier. Al-Waeli et al. [142] developed a photovoltaic thermal system to ameliorate the performance and reduce the number of required materials and parts and compared them with the proposed experimentally recorded values and modeled results. It was concluded that the electrical and thermal performance of the simulation and experimental results were 13.7% and 13.2%, and 72% and 71.3%, respectively. The overall efficiency was measured at 85.7%, and the peak photovoltaic panel temperature was observed to be 41.2 °C. The modeled outcomes were in good agreement with the experimentally obtained ones.

A novel approach of comparing the performance of a conventional photovoltaic system and a nanofluid photovoltaic/thermal system with a nanofluid–PCM-integrated system through experimental investigation was proposed by the authors Sardarabadi et al. [143]. For this purpose, monocrystalline silicon photovoltaic panels of 40 W for all alternatives were used outdoors in Mashhad, Iran, for several days in August and September. A zinc oxide aqueous nanofluid at 0.2% wt. flowing at 30 kg/h in a copper sheet and a tube collector attached to the rear of the photovoltaic panel were used. The employed PCM was paraffin wax with a melting point in the temperature range of between 42 °C and 72 °C, and it was positioned in the surroundings of the third system's tubes. The authors reported a maximum temperature decrease of approximately 7 °C and 16 °C for the nanofluid photovoltaic/thermal system and the nanofluid–PCM-integrated system, respectively, with respect to that of the conventional photovoltaic system. The PCM absorbed an additional

amount of heat from the photovoltaic panel in its latent heat, lowering and stabilizing the average surface temperature of the photovoltaic panel. The zinc oxide nanofluid also absorbed a considerable amount of heat because of its high thermal conductivity derived from the incorporation of nanoparticles, and this absorption of heat also resulted in enhanced thermal power. The increases in the electrical efficiency enhancements were of 8% and 23% for the system working with nanofluid and for the nanofluid–PCM-integrated system, respectively, in comparison to the traditional photovoltaic system. Hence, the research team concluded that the nanofluid–PCM operating system was the best performing one. Moreover, the researchers Al-Waeli et al. [144] determined the overall efficiency of a photovoltaic/thermal system using a nanofluid and a nano-enhanced PCM for the efficient cooling of the photovoltaics with a focus on improving the electrical efficiency. Silicon carbide nanoparticles were added to water and to paraffin wax. The nano-enhanced PCM was synthesized in an ultrasonic mixer with the addition of from 0.1% wt. to 4% wt. of silicon carbide. At 3% wt., the maximum thermal conductivity increase was reached, which, consequently, was the concentration used for the nano-enhanced PCM. Similarly, the prepared nanofluid also had a 3% mass fraction of SiC in water. The photovoltaic average surface temperature decreased with increasing flowrate in the copper tubes, with an imposed flow rate of 0.170 kg/s. The incorporation of the nanoparticles enhanced the heat transfer capability of both the water and the paraffin. The PCM first absorbed the extra photovoltaic panel heat and then transferred it to nanofluid flowing in tubes, leading to more heat extraction from the photovoltaic module. By simultaneously exploring a nanofluid and a nano-enhanced PCM in the photovoltaic/thermal system, a reduction in the temperature of the photovoltaic cell of around 17 °C was obtained. Also, this system provided an approximately 42.5% heat gain increase in comparison with a photovoltaic/thermal system operating with water and paraffin.

The combined use of nanofluids with PCMs has been an influential thermal management methodology for photovoltaic/thermal systems in the recent years. Many experimental works and numerical simulations have been performed in this area. PCMs together with nanofluids have been a very attractive alternative to researchers in comparison with other materials, mainly due to the synergistic effect derived from the enhanced thermal conductivity and diffusivity offered by nanofluids and the enhanced heat storage capability of PCMs. The latter are integrated with nanofluids to overcome the poor heat transfer coefficient and insufficient contact area problem associated with PCMs. Furthermore, the authors Salem et al. [4] studied the cooling effect provided by an alumina/PCM mixture on a photovoltaic thermal system. The researchers circulated the alumina/PCM mixture and/or water at nanoparticle concentrations of up to 1% wt. and mass fluxes of up to 5.31 kg/s.m^2 in aluminum channels underneath the photovoltaic cells. The authors stated that the cooling process using this compound solution performed better than cooling with ordinary water. The highest photovoltaic performance of 110% achieved with the mixture was translated into the highest photovoltaic electrical output. Additionally, the researchers Al-Waeli et al. [140] evaluated the thermal performance of a photovoltaic/thermal system deploying diverse heat transfer enhancement routes: a PCM with a silicon carbide nanofluid, a PCM and water, and only water. The authors found that the nano-enhanced PCM and the nanofluid compound solution enhanced the electrical efficiency from 8% to around 13.3% and the electrical current output from nearly 3.7% to 4% compared with those attained with a common photovoltaic/thermal system. Also, it should be emphasized that the authors arrived at a consistent comparison between the experimentally obtained results and the ones estimated through the artificial neural network, multilayer perceptron, and support vector machine methodologies. The proposed model results were compared with the experimental ones with coefficient of determination R2, MSE, and RMSE values of 0.99, 0.006, and 0.009, respectively. Similarly, the authors Al-Waeli et al. [144] proposed a hybrid photovoltaic/thermal system using a PCM and a nanofluid to enhance the overall efficiency of the system. The developed nano-enhanced PCM was one composed of paraffin with a dispersion of silicon carbide nanoparticles. The experiment was conducted

outdoors, employing a fluid flow rate of around 0.2 Kg/s. The electrical performance with this technological solution was enhanced from nearly 7% to 14%, the circuit voltage was enhanced from 11 V to 13 V to 20–21 V, and the power output increased from nearly 61 W to around 121 W. Also, there was a considerable cell temperature decrease, and the thermal efficiency reached 72%.

The authors Hassan et al. [137] reported on an experimental study on the simultaneous usage of a nanofluid and a PCM for thermal regulation in photovoltaic modules. The authors used an aqueous graphene nanofluid and a TR-35HC PCM with varying graphene nanostructure concentrations of 0.05% vol. to 0.15% vol., and different flow rates of between 20 L/min and 40 L/min. The authors found that the best thermal performance was attained using a graphene concentration of 0.1% vol. and a flow rate of 40 L/min. The average temperature decrease of the photovoltaic panels was of nearly 24 °C, 16 °C, and 12 °C with the system working with water and a PCM, a nano-enhanced PCM, and a PCM, respectively. The performance of the system employing a nano-enhanced PCM was improved by 12% with respect to that attained with water and a PCM, and the electrical efficiency was approximately 24% superior to the one for the common photovoltaic/thermal system. Furthermore, the authors Naghdbishi et al. [145] studied the combined effect of multi-walled carbon nanotubes dispersed in water nanofluid and paraffin wax on one hybrid photovoltaic/thermal PCM system. The maximum electrical energetic and exergetic efficiencies were attained in the cases where the multi-walled carbon nanotubes/water nanofluid was employed. The enhanced thermal fluid increased the electrical and thermal efficiencies of the system to nearly 4.2% and 23.6%, respectively, with respect to those obtained with a traditional photovoltaic module. Similarly, the researchers Salari et al. [146] elaborated a numerical simulation on a nanofluid photovoltaic/thermal system integrated with PCMs. In this direction, magnesium oxide nanoparticles, multi-walled carbon nanotubes, and a combination of both were added to water and used as working fluids. The obtained results showed that the surface temperature of the system using the multi-walled carbon nanotube nanofluid decreased by 0.3 °C when the concentration of the carbon nanotubes was increased from 3% wt. to 6% wt. Also, energy efficiencies of nearly 60.7%, 61.1%, 60.1%, and 55.2% were achieved using the hybrid form of the nanofluid, only multi-walled carbon nanotube fillers, only magnesium oxide fillers, and pure water, respectively. The authors also found that the outflow as well as the surface temperatures were diminished with the increase in the PCM layer thickness. Table 2 summarizes the fundamental recent published works on the simultaneous use of nanofluids and PCMs in photovoltaic/thermal systems.

Table 2. Main published works on the combined usage of nanofluids and PCMs in photovoltaic/thermal systems.

Authors	Nanofluid	Concentration	Phase-Change Material	Main Findings	Reference
Salem et al.	Alumina–water	Up to 1% wt.	Calcium chloride hexahydrate	The best performance was achieved with the compound cooling technique with an alumina–PCM mixture.	[4]
Abdelrahman et al.	Alumina–water	0.1 to 0.8% vol.	RT35HC	The mixture of the alumina nanoparticles into the RT35HC PCM with an increase in nanoparticle concentration from 0.11 to 0.77% vol. reduced the surface temperature of the photovoltaic cell by 53.2%.	[147]
Abdollahi and Rahimi	Boehmite–oil	0.9% wt.	Coconut oil/sunflower oil mixture	The highest efficiency was achieved using the nano-enhanced PCM with an increase in power output of up to 48.2%.	[148]
Hassan et al.	Graphene–water	0.05 to 0.15% vol.	RT35HC	The effectiveness of the nano-photovoltaic/thermal PCM device was 17.5% higher and the overall efficiency was 12% higher than those of the water photovoltaic/thermal PCM system.	[137]

Table 2. *Cont.*

Authors	Nanofluid	Concentration	Phase-Change Material	Main Findings	Reference
Al-Waeli et al.	Silicon carbide–water	0.1 to 4% wt.	Paraffin wax	Combined silicon carbide nanofluid and a nano-PCM was the best cooling option, with a 13.3% electrical efficiency compared with only 8.1% in the conventional photovoltaic system.	[141]
Al-Waeli et al.	Silicon carbide–water	0.1 to 4% wt.	Paraffin wax	The performance of the proposed combined nano-PCM and nanofluid photovoltaic/thermal system enhanced the electrical efficiency from 7.1% to 13.7%, the power from 61.1 W to 129.7 W, and the open-circuit voltage from 11 to 13 V to 20–21 V, and the thermal efficiency reached 72%.	[134]
Al-Waeli et al.	Silicon carbide–water	0.1 to 4% wt.	Paraffin wax	The technoeconomic evaluation of the nano-enhanced PCM and nanofluid-based PVT system revealed that the specific yield, the capacity factor, the efficiency of the inverter, the cost of electricity, and the payback period were 190.4 kWh/kWp, 25%, 97.3%, 0.125 USD/kWh, and 5–6 years, respectively. The ANN model findings were found to be consistent with those of recent published experimental works, demonstrating the reliability of this model.	[138]
Al-Waeli et al.	Silicon carbide–water	0.1 to 4% wt.	Paraffin wax	Proposition of linear projection models to reduce the error of the potential outcomes and determine the optimal conditions for every solar thermal energy system	[140]
Hosseinzadeh et al.	Zinc oxide–water		Paraffin wax	The overall exergy efficiencies of the photovoltaic, nanofluid photovoltaic, and nanofluid–PCM-integrated system were 10.7%, 13.6%, and 12.4%, respectively. There was a decrease in entropy generation of 1.6% and 3.2% in the nanofluid and nanofluid–PCM systems, respectively. An electrical power efficiency of 13.6% and a thermal power efficiency of 29.6% were attained.	[136]
Sardarabadi et al.	Zinc oxide–water		Paraffin wax	The photovoltaic/thermal system operating with a PCM and zinc oxide nanofluid had higher thermal, electrical, and overall efficiencies and more photovoltaic panel surface temperature reduction. It had a thermal power efficiency 46% greater than that of the photovoltaic system with water as a coolant.	[135]
Sarafraz et al.	MWCNTs–water	0.2% wt.	Paraffin wax	The best thermal and electrical performance was attained at 0.2% of the multi-walled carbon nanotubes for the nano-enhanced PCM and nanofluid. An electrical power efficiency of around 276 W/m^2 and a thermal power efficiency of around 308 W/m^2 were attained.	[139]

5.3. Thermal Management of Residential Buildings

To meet the ever-increasing thermal energy demands in the residential building universe, the researchers Lari and Sahin [149] developed an upgrade to a nanofluid photovoltaic/thermal retrofitting PCM thermal battery. The authors conducted daily and yearly technoeconomic analyses of the system using the Engineering Equation Solver (EES) software considering the annual performance of the system without heat storage and with uncooled photovoltaics. Compared to the uncooled photovoltaic systems, the researchers found an almost 12% increase in the electric output of the developed thermal battery and better thermal regulation in the photovoltaic panel. It was concluded that the proposed system could fulfil the power demand with 77% electrical power and 27.3% thermal power.

6. Limitations and Prospects for Further Research

The main limitations and prospects for further investigation into the combined use of PCMs and nanofluids for solar thermal heat transfer enhancement can be summarized in the following points:

- The technological approaches described herein are very promising but exhibit some disadvantages, including the absence of standard preparation methods for nanofluids and nano-enhanced PCMs and some inconsistencies in the measurement methodologies for the different factors to determine the behavior of PCMs. Moreover, nanofluids and nano-enhanced PCMs may have agglomeration and settling problems after only a limited number of cycles of operation. Additionally, some potential PCMs and nano-enhanced PCMs possess leakage problems inherent to the solid–liquid phase transition.

- There is a lack of knowledge and internationally recognized standards for monitoring and testing photovoltaic/thermal systems operating with nanofluids and PCMs simultaneously, which limits the growth of this technological approach.

- There is a very limited number of commercially available photovoltaic/thermal systems due to some key challenges that need to be overcome, such as their thermal and electrical efficiencies, long-term performance details, and the compatibility of the thermal systems with the different types of photovoltaic panels. This may hinder improved knowledge of the practical technical design limitations and long-term real-life reliability studies of photovoltaic/thermal systems in general and of those assisted with the combined employment of nanofluids and PCMs.

- Further experimental works should be conducted and more accurate preparation routes should be developed for thermal management systems using PCMs and nanofluids. In the available published studies about this hybrid heat transfer route, some relevant details are still missing for the sake of the repeatability of the results and representative sampling, including the different types of base fluids and optimal concentration of nanofluids, synthesis methodologies, and safety procedures.

- A limited number of researchers investigating PCMs have carried out specific heat determination. Additionally, the scarce experimental works regarding the specific heat are not consistent with each other, normally presenting considerable variations. In some of the published studies, the specific heat of PCMs increased with increasing concentration of nanoparticles, and in others, the opposite evolution was observed. Considering these facts, further studies on the specific heat capacity of PCMs and the influencing factors are most welcome.

- The major concerns about the synthesis, characterization, and employment of PCMs together with nanofluids are the initial investment cost and the inherent economic analysis. Nonetheless, the economic viability and overall cost are issues that have still not yet been sufficiently addressed, and, consequently, further in-depth studies on the subject are needed.

- It is highly recommended to conduct further analysis on the environmental impact of nanofluid and phase-change material combinations to acquire enriched knowledge on the topic. Most of the scientific articles lack an explanation of the environmental impact in the synthesis, utilization, and final disposal stages of these materials. Also, the available literature does not present extensive guidelines for the safety procedures associated with the handling, use, and characterization of nanofluids and PCMs. Hence, it is strongly suggested to publish an environmental impact evaluation through life cycle assessment analysis and a description of the safety procedures to ensure a safe working environment for the researchers and potential users of nanofluids and PCMs.

- Additional issues that should be addressed include the need for a decrease in the cost of PCM synthesis methods and active equipment and the thermal stability and stability over time of nanofluids explored in solar thermal energy systems.

- Most of the PCMs employed in the technological area of solar energy storage and conversion are single materials like, for instance, paraffin waxes, and, consequently, further experimental works involving mixtures of different PCMs along with the use of nanofluids should be carried out. These works would provide useful insights into the synergistic benefits coming from the high thermal energy storage density and stability of such mixtures.

- The high-grade exergy and environmental effects of the developed photovoltaics/thermal systems with the combined usage of nanofluids and PCMs should be evaluated. For this purpose, it is suggested to conduct further life cycle investigation and comparison analysis between the conventional and enhanced systems. Such studies would enable the determination of the accumulated exergies and carbon dioxide emissions during the diverse working stages of the system's lifespan.

- The search for more environmentally friendly PCMs with less toxicity should be continued. Also, one of the future research topics should address attempts to improve the thermal properties of PCMs, namely, their relatively poor thermal conductivity.

7. Conclusions

The main concluding remarks of this review on the combined usage of nanofluids and PCMs in energy storage and conversion systems are highlighted in the following points:

- PCMs and nanofluids are very suitable to being applied in solar energy recovery systems because of their intrinsic beneficial features like improved thermal stability, recyclability, and lack of supercooling. Hence, it is predictable that the improved thermal energy storage equipment and systems using PCMs and nanofluids simultaneously will have an important role in future thermal solar energy conversion and harvesting processes.

- The combination of PCMs and nanofluids is the most effective photovoltaic thermal management choice with respect to the separated contribution of PCMs and nanofluids because of the additional heat dissipation of photovoltaic panels. Improved solar thermal energy management is attained in cases where nanofluid is used simultaneously with a nano-enhanced PCM and used as working fluid in photovoltaic/thermal systems.

- The combined usage of nanofluids and PCMs appreciably increases the thermal energy storage capacity and extends the working time of solar thermal energy storage systems considerably. Also, photovoltaic/thermal systems using nanofluids and PCMs simultaneously can considerably reduce the overreliance on fossil fuels to produce electricity and decrease carbon dioxide and greenhouse gas emissions.

- The simultaneous exploration of nanofluids and PCMs significantly increases the thermal conductivity and diffusivity and the convective heat transfer coefficient of photovoltaic/thermal systems. These benefits entail much lower convective and radiant losses derived from the overall improvement of the heat transfer performance. Nonetheless, it should be noted that increasing the concentration of the nanoparticles in the nanofluids increases the viscosity and pressure drops of the solar thermal system, requiring additional pumping power, which results in a higher overall investment cost of the produced electricity.

- The combined usage of nanofluids and PCMs has proven to be more effective for photovoltaic/thermal systems cooling than the individual exploration of either PCMs or nanofluids. Such a synergetic route normally gives rise to extra heat removal capability for photovoltaic panels because the heat is extracted in sequence by the PCM and nanofluid. The combination of the PCM and nanofluid lowers the surface temperature and, at the same time, improves the temperature uniformity of the photovoltaic panels. Such effects mainly derive from the uniform contact of the PCM with the panels.

- The not-converted incident thermal solar energy in photovoltaic/thermal systems can be stored by PCMs in the form of latent heat, which may reduce the average surface temperature of the panels by more than 30 °C. Additionally, the adoption of a particular PCM should be based on many factors, including the environment typical temperature

values and latitude, solar irradiation intensity, and wind velocity, among others, given that the effectiveness of a PCM is more intense during the summer than the winter because the PCM absorbs more heat in summer, leading to an increased efficiency.

- The thermal performance of photovoltaic/thermal systems using PCMs and nanofluids simultaneously can be improved with different approaches, using, for instance, different PCMs, nanoparticles and base fluids, flow rates, channel configurations, operating fluid inlet temperatures, and heat dissipation methodologies of photovoltaic panels. An extra measure could be the jet impingement of nanofluids for the thermal management of photovoltaic panels and to extract a great quantity of energy in the form of heat.
- The increase in the overall electrical efficiency and thermal performance of photovoltaic/thermal systems may lead to a reduction in the corresponding payback periods. Innovative methods like the tolerance capital cost method accurately predict the economic feasibility of photovoltaic/thermal systems. Nonetheless, negative effects like the deposition over time of dust on photovoltaic panels can diminish the output of the system's life cycle cost.
- PCMs should be carefully selected to operate in photovoltaic/thermal systems installed in areas with hot climates. In these cases, among the diverse possibilities, salt hydrates have already been demonstrated to perform better and make the systems technically and financially viable when implemented in hot climates.
- The artificial neural network, multilayer perceptron, and support vector machine predicting methodologies can be explored for an accurate estimation of the efficiencies of photovoltaic/thermal systems employing PCMs and nanofluids. These methodologies are also very useful for optimizing the operating parameters of the systems to attain superior thermal performance.

Author Contributions: Conceptualization, J.P. and R.S.; methodology, J.P. and A.M. (Ana Moita); software, A.M. (Ana Moita); validation, A.M. (Ana Moita) and A.M. (António Moreira); formal analysis, A.M. (Ana Moita); investigation, J.P. and R.S.; resources, A.M. (António Moreira); data curation, J.P. and R.S.; writing—original draft preparation, J.P. and R.S.; writing—review and editing, J.P. and R.S.; supervision, A.M. (Ana Moita) and A.M. (António Moreira); project administration, A.M. (António Moreira); funding acquisition, A.M. (António Moreira). All authors have read and agreed to the published version of the manuscript.

Institutional Review Board Statement: Not applicable.

Informed Consent Statement: Not applicable.

Data Availability Statement: Data sharing is not applicable.

Conflicts of Interest: The authors declare no conflict of interest.

Sample Availability: Not applicable.

References

1. Nourafkan, E.; Asachi, M.; Jin, H.; Wen, D.; Ahmed, W. Stability and Photo-Thermal Conversion Performance of Binary Nanofluids for Solar Absorption Refrigeration Systems. *Renew. Energy* **2019**, *140*, 264–273. [CrossRef]
2. Siddique, R.M.A.; Kratz, F.; Mahmud, S.; Van Heyst, B. Energy Conversion by Nanomaterial-Based Trapezoidal-Shaped Leg of Thermoelectric Generator Considering Convection Heat Transfer Effect. *J. Energy Resour. Technol.* **2019**, *141*, 082001. [CrossRef]

3. Natividade, P.S.G.; de Moraes Moura, G.; Avallone, E.; Bandarra Filho, E.P.; Gelamo, R.V.; Gonçalves, J.C.d.S.I. Experimental Analysis Applied to an Evacuated Tube Solar Collector Equipped with Parabolic Concentrator Using Multilayer Graphene-Based Nanofluids. *Renew. Energy* **2019**, *138*, 152–160. [CrossRef]

4. Salem, M.; Elsayed, M.; Abd-Elaziz, A.; Elshazly, K. Performance enhancement of the photovoltaic cells using Al_2O_3/PCM mixture and/or water cooling-techniques. *Renew. Energy* **2019**, *138*, 876–890. [CrossRef]

5. Martín, M.; Villalba, A.; Inés Fernández, A.; Barreneche, C. Development of New Nano-Enhanced PCMs (NEPCM) to Improve Energy Efficiency in Buildings: Lab-Scale Characterization. *Energy Build.* **2019**, *192*, 75–83. [CrossRef]

6. Ren, Q.; Xu, H.; Luo, Z. PCM Charging Process Accelerated with Combination of Optimized Triangle Fins and Nanoparticles. *Int. J. Therm. Sci.* **2019**, *140*, 466–479. [CrossRef]

7. Balakin, B.V.; Zhdaneev, O.V.; Kosinska, A.; Kutsenko, K.V. Direct Absorption Solar Collector with Magnetic Nanofluid: CFD Model and Parametric Analysis. *Renew. Energy* **2019**, *136*, 23–32. [CrossRef]

8. Bonab, H.B.; Javani, N. Investigation and Optimization of Solar Volumetric Absorption Systems Using Nanoparticles. *Sol. Energy Mater. Sol. Cells* **2019**, *194*, 229–234. [CrossRef]

9. Wang, L.; Zhu, G.; Wang, M.; Yu, W.; Zeng, J.; Yu, X.; Xie, H.; Li, Q. Dual Plasmonic Au/TiN Nanofluids for Efficient Solar Photothermal Conversion. *Sol. Energy* **2019**, *184*, 240–248. [CrossRef]

10. Zhang, J.J.; Qu, Z.G.; Maharjan, A. Numerical Investigation of Coupled Optical-Electrical-Thermal Processes for Plasmonic Solar Cells at Various Angles of Incident Irradiance. *Energy* **2019**, *174*, 110–121. [CrossRef]

11. Zayed, M.E.; Zhao, J.; Du, Y.; Kabeel, A.E.; Shalaby, S.M. Factors Affecting the Thermal Performance of the Flat Plate Solar Collector Using Nanofluids: A Review. *Sol. Energy* **2019**, *182*, 382–396. [CrossRef]

12. Abdelrazik, A.S.; Al-Sulaiman, F.A.; Saidur, R.; Ben-Mansour, R. Evaluation of the Effects of Optical Filtration and NanoPCM on the Performance of a Hybrid Photovoltaic-Thermal Solar Collector. *Energy Convers. Manag.* **2019**, *195*, 139–156. [CrossRef]

13. Agresti, F.; Fedele, L.; Rossi, S.; Cabaleiro, D.; Bobbo, S.; Ischia, G.; Barison, S. Nano-Encapsulated PCM Emulsions Prepared by a Solvent-Assisted Method for Solar Applications. *Sol. Energy Mater. Sol. Cells* **2019**, *194*, 268–275. [CrossRef]

14. Sheikholeslami, M.; Mahian, O. Enhancement of PCM Solidification Using Inorganic Nanoparticles and an External Magnetic Field with Application in Energy Storage Systems. *J. Clean. Prod.* **2019**, *215*, 963–977. [CrossRef]

15. De Matteis, V.; Cannavale, A.; Martellotta, F.; Rinaldi, R.; Calcagnile, P.; Ferrari, F.; Ayr, U.; Fiorito, F. Nano-Encapsulation of PCMs: From Design to Thermal Performance, Simulations and Toxicological Assessment. *Energy Build.* **2019**, *188–189*, 1–11. [CrossRef]

16. Altohamy, A.A.; Abd Rabbo, M.F.; Sakr, R.Y.; Attia, A.A. Effect of water based Al_2O_3 nanoparticle PCM on cool storage performance. *Appl. Therm. Eng.* **2015**, *84*, 331–338. [CrossRef]

17. Shao, X.-F.; Mo, S.-P.; Chen, Y.; Yin, T.; Yang, Z.; Jia, L.-S.; Cheng, Z.-D. Solidification behavior of hybrid TiO_2 nanofluids containing nanotubes and nanoplatelets for cold thermal energy storage. *Appl. Therm. Eng.* **2017**, *117*, 427–436. [CrossRef]

18. Philip, J.; Shima, P.D. Thermal properties of nanofluids. *Adv. Colloid Interface Sci.* **2012**, *183*, 30–45. [CrossRef]

19. Ouabouch, O.; Kriraa, M.; Lamsaadi, M. Stability, Thermophysical Properties of Nanofluids, and Applications in Solar Collectors: A Review. *AIMS Mater. Sci.* **2021**, *8*, 659–684. [CrossRef]

20. Pinto, R.V.; Fiorelli, F.A.S. Review of the Mechanisms Responsible for Heat Transfer Enhancement Using Nanofluids. *Appl. Therm. Eng.* **2016**, *108*, 720–739. [CrossRef]

21. Gonçalves, I.; Souza, R.; Coutinho, G.; Miranda, J.; Moita, A.; Pereira, J.E.; Moreira, A.; Lima, R. Thermal Conductivity of Nanofluids: A Review on Prediction Models, Controversies and Challenges. *Appl. Sci.* **2021**, *11*, 2525. [CrossRef]

22. Lomascolo, M.; Colangelo, G.; Milanese, M.; de Risi, A. Review of Heat Transfer in Nanofluids: Conductive, Convective and Radiative Experimental Results. *Renew. Sustain. Energy Rev.* **2015**, *43*, 1182–1198. [CrossRef]

23. Souza, R.R.; Gonçalves, I.M.; Rodrigues, R.O.; Minas, G.; Miranda, J.M.; Moreira, A.L.N.; Lima, R.; Coutinho, G.; Pereira, J.E.; Moita, A.S. Recent Advances on the Thermal Properties and Applications of Nanofluids: From Nanomedicine to Renewable Energies. *Appl. Therm. Eng.* **2022**, *201*, 117725. [CrossRef]

24. Ambreen, T.; Kim, M.-H. Influence of Particle Size on the Effective Thermal Conductivity of Nanofluids: A Critical Review. *Appl. Energy* **2020**, *264*, 114684. [CrossRef]

25. Qiu, L.; Zhu, N.; Feng, Y.; Michaelides, E.E.; Żyła, G.; Jing, D.; Zhang, X.; Norris, P.M.; Markides, C.N.; Mahian, O. A Review of Recent Advances in Thermophysical Properties at the Nanoscale: From Solid State to Colloids. *Phys. Rep.* **2020**, *843*, 1–81. [CrossRef]

26. Ghadimi, A.; Saidur, R.; Metselaar, H.S.C. A Review of Nanofluid Stability Properties and Characterization in Stationary Conditions. *Int. J. Heat Mass Transf.* **2011**, *54*, 4051–4068. [CrossRef]

27. Jia-Fei, Z.; Zhong-Yang, L.; Ming-Jiang, N.; Ke-Fa, C. Dependence of Nanofluid Viscosity on Particle Size and PH Value. *Chin. Phys. Lett.* **2009**, *26*, 66202. [CrossRef]

28. Hwang, Y.; Lee, J.-K.; Lee, J.-K.; Jeong, Y.-M.; Cheong, S.; Ahn, Y.-C.; Kim, S.H. Production and Dispersion Stability of Nanoparticles in Nanofluids. *Powder Technol.* **2008**, *186*, 145–153. [CrossRef]

29. Hwang, Y.; Lee, J.K.; Lee, C.H.; Jung, Y.M.; Cheong, S.I.; Lee, C.G.; Ku, B.C.; Jang, S.P. Stability and Thermal Conductivity Characteristics of Nanofluids. *Thermochim. Acta* **2007**, *455*, 70–74. [CrossRef]

30. Mohammadpoor, M.; Sabbaghi, S.; Zerafat, M.M.; Manafi, Z. Investigating heat transfer properties of copper nanofluid in ethylene glycol synthesized through single and two-step routes. *Int. J. Refrig.* **2019**, *99*, 243–250. [CrossRef]

31. Kiani, M.R.; Meshksar, M.; Makarem, M.A.; Rahimpour, M.R. Chapter 2—Preparation, stability, and characterization of nanofluids. In *Nanofluids and Mass Transfer*; Rahimpour, M.R., Makarem, M.A., Kiani, M.R., Sedghamiz, M.A., Eds.; Elsevier: Amsterdam, The Netherlands, 2022; pp. 21–38. [CrossRef]

32. Lizana, J.; Chacartegui, R.; Barrios-Padura, A.; Valverde, J.M. Advances in Thermal Energy Storage Materials and Their Applications towards Zero Energy Buildings: A Critical Review. *Appl. Energy* **2017**, *203*, 219–239. [CrossRef]

33. Yang, X.H.; Huang, C.H.; Ke, H.B.; Chen, L.; Song, P. Evaluation of Thermal Control Performance of PCMs for Thermal Shock Protection of Electronics. *J. Phys. Conf. Ser.* **2021**, *2045*, 12032. [CrossRef]

34. Choi, D.H.; Lee, J.; Hong, H.; Kang, Y.T. Thermal conductivity and heat transfer performance enhancement of phase change materials (PCM) containing carbon additives for heat storage application. *Int. J. Refrig.* **2014**, *42*, 112–120. [CrossRef]

35. Wang, J.; Xie, H.; Xin, Z.; Li, Y.; Chen, L. Enhancing thermal conductivity of palmitic acid based phase change materials with carbon nanotubes as fillers. *Sol. Energy* **2010**, *84*, 339–344. [CrossRef]

36. Yu, Z.; Fang, X.; Fan, L.; Wang, X.; Xiao, Y.; Zeng, Y.; Xu, X.; Hu, Y.; Cen, K. Increased thermal conductivity of liquid paraffinbased suspensions in the presence of carbon nano-additives of various sizes and shapes. *Carbon* **2013**, *53*, 277–285. [CrossRef]

37. Li, M. A nano-graphite/paraffin phase change material with high thermal conductivity. *Appl. Energy* **2013**, *106*, 25–30. [CrossRef]

38. Li, Y.; Li, J.; Deng, Y.; Guan, W.; Wang, X.; Qian, T. Preparation of paraffin/porous TiO_2 foams with enhanced thermal conductivity as PCM, by covering the TiO_2 surface with a carbon layer. *Appl. Energy* **2016**, *171*, 37–45. [CrossRef]

39. Chen, Y.; Luo, W.; Wang, J.; Huang, J. Enhanced thermal conductivity and durability of a paraffin wax nanocomposite based on carbon-coated aluminum nanoparticles. *J. Phys. Chem. C* **2017**, *121*, 12603–12609. [CrossRef]

40. Cheng, F.; Wen, R.; Huang, Z.; Fang, M.; Liu, Y.; Wu, X.; Min, X. Preparation and analysis of lightweight wall material with expanded graphite (EG)/paraffin composites for solar energy storage. *Appl. Therm. Eng.* **2017**, *120*, 107–114. [CrossRef]

41. Seki, Y.; Ince, S.; Ezan, M.A.; Turgut, A.; Erek, A. Graphite nanoplates loading into eutectic mixture of Adipic acid and Sebacic acid as phase change material. *Sol. Energy Mater. Sol. Cells* **2015**, *140*, 457–463. [CrossRef]

42. Huang, Y.; Hsieh, T.E. Effective thermal parameters of chalcogenide thin films and simulation of phase-change memory. *Int. J. Therm. Sci.* **2015**, *87*, 207–214. [CrossRef]

43. Qiu, L.; Zheng, X.; Su, G.; Tang, D. Design and application of a freestanding sensor based on 3ω technique for thermal-conductivity measurement of solids, liquids, and nanopowders. *Int. J. Thermophys.* **2013**, *34*, 2261–2275. [CrossRef]

44. Gharebaghi, M.; Sezai, I. Enhancement of heat transfer in latent heat storage modules with internal fins. *Numer. Heat Transf. Part A* **2008**, *53*, 749–765. [CrossRef]

45. Castell, A.; Sole, C.; Medrano, M.; Roca, J.; Cabeza, L.F.; Garcia, D. Natural convection heat transfer coefficients in phase change material (PCM) modules with external vertical fins. *Appl. Therm. Eng.* **2008**, *28*, 1676–1686. [CrossRef]

46. Nayak, K.C.; Saha, S.K.; Srinivasan, K.; Dutta, P. A numerical model for heat sinks with phase change materials and thermal conductivity enhancers. *Int. J. Heat Mass Transf.* **2006**, *49*, 1833–1844. [CrossRef]

47. Zhao, C.Y.; Lu, W.; Tian, Y. Heat transfer enhancement for thermal energy storage using metal foams embedded within phase change materials (PCMs). *Solar Energy* **2010**, *84*, 1402–1412. [CrossRef]

48. Ettouney, H.M.; Alatiqi, I.; Al-Sahali, M.; Al-Hajirie, K. Heat transfer enhancement in energy storage in spherical capsules filled with paraffin wax and metal beads. *Energy Convers. Manag.* **2006**, *47*, 211–228. [CrossRef]

49. Sari, A.; Karaipekli, A. Preparation, thermal properties and thermal reliability of palmitic acid/expanded graphite composite as form-stable PCM for thermal energy storage. *Sol. Energy Mater. Sol. Cells* **2009**, *93*, 571–576. [CrossRef]

50. Rao, Z.H.; Zhang, G.Q. Thermal Properties of Paraffin Wax-based Composites Containing Graphite. *Energy Sources Part A* **2011**, *33*, 587–593. [CrossRef]

51. Wang, Y.; Xia, T.D.; Feng, H.X.; Zhang, H. Stearic acid/polymethylmethacrylate composite as form-stable phase change materials for latent heat thermal energy storage. *Renew. Energy* **2011**, *36*, 1814–1820. [CrossRef]

52. Jegadheeswaran, S.; Pohekar, S.D. Performance enhancement in latent heat thermal storage system: A review. *Renew. Sustain. Energy Rev.* **2009**, *13*, 2225–2244. [CrossRef]

53. Seeniraj, R.V.; Narasimhan, N.L. Performance enhancement of a solar dynamic LHTS module having both fins and multiple PCMs. *Sol. Energy* **2008**, *82*, 535–542. [CrossRef]

54. Shaikh, S.; Lafdi, K. Effect of multiple phase change materials (PCMs) slab configurations on thermal energy storage. *Energy Convers. Manag.* **2006**, *47*, 2103–2117. [CrossRef]

55. Cui, H.; Yuan, X.; Hou, X. Thermal performance analysis for a heat receiver using multiple phase change materials. *Appl. Therm. Eng.* **2003**, *23*, 2353–2361. [CrossRef]

56. Hawlader, M.N.A.; Uddin, M.S.; Khin, M.M. Microencapsulated PCM thermal-energy storage system. *Appl. Energy* **2003**, *74*, 195–202. [CrossRef]

57. Sari, A.; Alkan, C.; Karaipekli, A. Preparation, characterization and thermal properties of PMMA/n-heptadecane microcapsules as novel solid–liquid microPCM for thermal energy storage. *Appl. Energy* **2010**, *87*, 1529–1534. [CrossRef]

58. Muzhanje, A.T.; Hassan, M.A.; Ookawara, S.; Hassan, H. An Overview of the Preparation and Characteristics of PCMs with Nanomaterials. *J. Energy Storage* **2022**, *51*, 104353. [CrossRef]

59. Yadav, A.; Barman, B.; Kumar, V.; Kardam, A.; Shankara Narayanan, S.; Verma, A.; Madhwal, D.; Shukla, P.; Jain, V.K. *A Review on Thermophysical Properties of Nanoparticle-Enhanced PCMs for Thermal Energy Storage BT—Recent Trends in Materials and Devices*; Jain, V.K., Rattan, S., Verma, A., Eds.; Springer International Publishing: Cham, Switzerland, 2017; pp. 37–47.

60. Fullenkamp, K.; Montané, M.; Cáceres, G.; Araya-Letelier, G. Review and Selection of EPCM as TES Materials for Building Applications. *Int. J. Sustain. Energy* **2019**, *38*, 561–582. [CrossRef]
61. Kahwaji, S.; White, M.A. Edible Oils as Practical PCMs for Thermal Energy Storage. *Appl. Sci.* **2019**, *9*, 1627. [CrossRef]
62. Boussaba, L.; Makhlouf, S.; Foufa, A.; Lefebvre, G.; Royon, L. Vegetable Fat: A Low-Cost Bio-Based PCM for Thermal Energy Storage in Buildings. *J. Build. Eng.* **2019**, *21*, 222–229. [CrossRef]
63. Wonorahardjo, S.; Sutjahja, I.M.; Kurnia, D.; Fahmi, Z.; Putri, W.A. Potential of Thermal Energy Storage Using Coconut Oil for Air Temperature Control. *Buildings* **2018**, *8*, 95. [CrossRef]
64. Da Cunha, S.R.L.; de Aguiar, J.L.B. PCMs and Energy Efficiency of Buildings: A Review of Knowledge. *J. Energy Storage* **2020**, *27*, 101083. [CrossRef]
65. Al-Yasiri, Q.; Szabó, M. Incorporation of PCMs into Building Envelope for Thermal Comfort and Energy Saving: A Comprehensive Analysis. *J. Build. Eng.* **2021**, *36*, 102122. [CrossRef]
66. Akeiber, H.; Nejat, P.; Majid, M.Z.A.; Wahid, M.A.; Jomehzadeh, F.; Zeynali Famileh, I.; Calautit, J.K.; Hughes, B.R.; Zaki, S.A. A Review on PCM (PCM) for Sustainable Passive Cooling in Building Envelopes. *Renew. Sustain. Energy Rev.* **2016**, *60*, 1470–1497. [CrossRef]
67. Das, S.S.; Kumar, P.; Sandhu, S.S. Hybrid Photovoltaic-Thermal Systems Utilizing Liquid-Gas PCM. Energy Sources, Part A Recover. *Util. Environ. Eff.* **2021**, *43*, 2896–2914. [CrossRef]
68. Kong, W.; Fu, X.; Liu, Z.; Zhou, C.; Lei, J. A Facile Synthesis of Solid-Solid PCM for Thermal Energy Storage. *Appl. Therm. Eng.* **2017**, *117*, 622–628. [CrossRef]
69. Du, X.; Qiu, J.; Deng, S.; Du, Z.; Cheng, X.; Wang, H. Flame-Retardant and Solid-Solid Phase Change Composites Based on Dopamine-Decorated BP Nanosheets/Polyurethane for Efficient Solar-to-Thermal Energy Storage. *Renew. Energy* **2021**, *164*, 1–10. [CrossRef]
70. Sikiru, S.; Oladosu, T.L.; Amosa, T.I.; Kolawole, S.Y.; Soleimani, H. Recent advances and impact of PCMs on solar energy: A comprehensive review. *J. Energy Storage* **2022**, *53*, 105200. [CrossRef]
71. Lebedev, V.A.; Amer, A.E. Limitations of using PCMs for thermal energy storage. *IOP Conf. Ser. Earth Environ. Sci.* **2019**, *378*, 012044. [CrossRef]
72. Philip, J.; Shima, P.D.; Raj, B. Evidence for Enhanced Thermal Conduction through Percolating Structures in Nanofluids. *Nanotechnology* **2008**, *19*, 305706. [CrossRef]
73. Chon, C.H.; Kihm, K.D.; Lee, S.P.; Choi, S.U.; Chon, C.H.; Kihm, K.D. Empirical correlation finding the role of temperature and particle size for nanofluid (Al_2O_3) thermal conductivity enhancement. *Appl. Phys. Lett.* **2005**, *87*, 153107. [CrossRef]
74. Beck, M.P.; Yuan, Y.; Warrier, P.; Teja, A.S. The Effect of Particle Size on the Thermal Conductivity of Alumina Nanofluids. *J. Nanoparticle Res.* **2009**, *11*, 1129–1136. [CrossRef]
75. Jeong, J.; Li, C.; Kwon, Y.; Lee, J.; Kim, S.H.; Yun, R. Particle Shape Effect on the Viscosity and Thermal Conductivity of ZnO Nanofluids. *Int. J. Refrig.* **2013**, *36*, 2233–2241. [CrossRef]
76. Murshed, S.M.S. Simultaneous Measurement of Thermal Conductivity, Thermal Diffusivity, and Specific Heat of Nanofluids. *Heat Transf. Eng.* **2012**, *33*, 722–731. [CrossRef]
77. Zhu, H.; Zhang, C.; Liu, S.; Tang, Y.; Yin, Y. Effects of Nanoparticle Clustering and Alignment on Thermal Conductivities of Fe_3O_4 Aqueous Nanofluids. *Appl. Phys. Lett.* **2006**, *89*, 23123. [CrossRef]
78. Hong, T.-K.; Yang, H.-S.; Choi, C.J. Study of the Enhanced Thermal Conductivity of Fe Nanofluids. *J. Appl. Phys.* **2005**, *97*, 064311. [CrossRef]
79. Dadwal, A.; Joy, P.A. Particle Size Effect in Different Base Fluids on the Thermal Conductivity of Fatty Acid Coated Magnetite Nanofluids. *J. Mol. Liq.* **2020**, *303*, 112650. [CrossRef]
80. Kamalvand, M.; Karami, M. A Linear Regularity between Thermal Conductivity Enhancement and Fluid Adsorption in Nanofluids. *Int. J. Therm. Sci.* **2013**, *65*, 189–195. [CrossRef]
81. Altan, C.L.; Gurten, B.; Sommerdijk, N.A.J.M.; Bucak, S. Deterioration in Effective Thermal Conductivity of Aqueous Magnetic Nanofluids. *J. Appl. Phys.* **2014**, *116*, 224904. [CrossRef]
82. Colla, L.; Fedele, L.; Mancin, S.; Danza, L.; Manca, O. Nano-PCMs for Enhanced Energy Storage and Passive Cooling Applications. *Appl. Therm. Eng.* **2017**, *110*, 584–589. [CrossRef]
83. Harish, S.; Orejon, D.; Takata, Y.; Kohno, M. Thermal Conductivity Enhancement of Lauric Acid Phase Change Nanocomposite with Graphene Nanoplatelets. *Appl. Therm. Eng.* **2015**, *80*, 205–211. [CrossRef]
84. Sarı, A.; Biçer, A.; Hekimoğlu, G. Effects of Carbon Nanotubes Additive on Thermal Conductivity and Thermal Energy Storage Properties of a Novel Composite PCM. *J. Compos. Mater.* **2018**, *53*, 2967–2980. [CrossRef]
85. Yadav, A.; Barman, B.; Kardam, A.; Narayanan, S.S.; Verma, A.; Jain, V.K. Thermal Properties of Nano-Graphite-Embedded Magnesium Chloride Hexahydrate Phase Change Composites. *Energy Environ.* **2017**, *28*, 651–660. [CrossRef]
86. Sharma, R.K.; Ganesan, P.; Tyagi, V.V.; Metselaar, H.S.C.; Sandaran, S.C. Thermal Properties and Heat Storage Analysis of Palmitic Acid-TiO_2 Composite as Nano-Enhanced Organic PCM (NEOPCM). *Appl. Therm. Eng.* **2016**, *99*, 1254–1262. [CrossRef]
87. Vivekananthan, M.; Amirtham, V.A. Characterization and Thermophysical Properties of Graphene Nanoparticles Dispersed Erythritol PCM for Medium Temperature Thermal Energy Storage Applications. *Thermochim. Acta* **2019**, *676*, 94–103. [CrossRef]
88. Putra, N.; Amin, M.; Kosasih, E.A.; Luanto, R.A.; Abdullah, N.A. Characterization of the Thermal Stability of RT 22 HC/Graphene Using a Thermal Cycle Method Based on Thermoelectric Methods. *Appl. Therm. Eng.* **2017**, *124*, 62–70. [CrossRef]

89. Nourani, M.; Hamdami, N.; Keramat, J.; Moheb, A.; Shahedi, M. Thermal Behavior of Paraffin-Nano-Al2O3 Stabilized by Sodium Stearoyl Lactylate as a Stable PCM with High Thermal Conductivity. *Renew. Energy* **2016**, *88*, 474–482. [CrossRef]

90. Wang, F.; Liu, J.; Fang, X.; Zhang, Z. Graphite Nanoparticles-Dispersed Paraffin/Water Emulsion with Enhanced Thermal-Physical Property and Photo-Thermal Performance. *Sol. Energy Mater. Sol. Cells* **2016**, *147*, 101–107. [CrossRef]

91. Zhou, S.Q.; Ni, R. Measurement of the specific heat capacity of water-based Al_2O_3 nanofluid. *Appl. Phys. Lett.* **2008**, *92*, 093123. [CrossRef]

92. O'Hanley, H.; Buongiorno, J.; McKrell, T.; Hu, L.W. Measurement and model correlation of specific heat capacity of water-based nanofluids with silica, alumina and copper oxide nanoparticles. *ASME Int. Mech. Eng. Congr. Expo.* **2011**, *54969*, 1209–1214.

93. Vajjha, R.S.; Das, D.K. Specific heat measurement of three nanofluids and development of new correlations. *J. Heat Transfer.* **2009**, *131*, 071601. [CrossRef]

94. O'Hanley, H.; Buongiorno, J.; McKrell, T.; Hu, L.W. Measurement and model validation of nanofluid specific heat capacity with differential scanning calorimetry. *Adv. Mech. Eng.* **2012**, *4*, 181079. [CrossRef]

95. Barbés, B.; Páramo, R.; Blanco, E.; Casanova, C. Thermal conductivity and specific heat capacity measurements of CuO nanofluids. *J. Therm. Anal. Calorim.* **2014**, *115*, 1883–1891. [CrossRef]

96. Teng, T.P.; Lin, L.; Yu, C.C. Preparation and Characterization of Carbon Nanofluids by Using a Revised Water-Assisted Synthesis Method. *J. Nanomater.* **2013**, *2013*, 133. [CrossRef]

97. De Robertis, E.; Cosme, E.H.H.; Neves, R.S.; Kuznetsov, A.Y.; Campos, A.P.C.; Landi, S.M.; Achete, C.A. Application of the modulated temperature differential scanning calorimetry technique for the determination of the specific heat of copper nanofluids. *Appl Therm Eng* **2012**, *41*, 10–17. [CrossRef]

98. Starace, A.K.; Gomez, J.C.; Wang, J.; Pradhan, S.; Glatzmaier, G.C. Nanofluid heat capacities. *J. Appl. Phys.* **2011**, *110*, 124323. [CrossRef]

99. Lin, Y.S.; Hsiao, P.Y.; Chieng, C.C. Roles of nanolayer and particle size on thermophysical characteristics of ethylene glycol-based copper nanofluids. *Appl. Phys. Lett.* **2011**, *98*, 153105. [CrossRef]

100. Wang, C.; Lin, T.; Li, N.; Zheng, H. Heat transfer enhancement of phase change composite material: Copper foam/paraffin. *Renew. Energy* **2016**, *96*, 960–965. [CrossRef]

101. Han, P.; Zheng, X.; Hou, W.; Qiu, L.; Tang, D. Study on heat-storage and release characteristics of multi-cavity-structured phase change microcapsules. *Phase Transit.* **2015**, *88*, 704–715. [CrossRef]

102. Babuska, I.; Szabo, B.A.; Katz, I.N. The p-version of the finite element method. *SIAM J. Numer. Anal.* **1981**, *18*, 515–545. [CrossRef]

103. Reddy, J. *An Introduction to the Finite Element Method*; McGraweHill: New York, NY, USA, 2013.

104. Wang, G.; Wei, G.; Xu, C.; Ju, X.; Yang, Y.; Du, X. Numerical simulation of effective thermal conductivity and pore-scale melting process of PCMs in foam metals. *Appl. Therm. Eng.* **2019**, *147*, 464–472. [CrossRef]

105. Lohrasbi, S.; Sheikholeslami, M.; Ganji, D.D. Multi-objective RSM optimization of fin assisted latent heat thermal energy storage system based on solidification process of phase change Material in presence of copper nanoparticles. *Appl. Therm. Eng.* **2017**, *118*, 430–447. [CrossRef]

106. Mahdi, J.M.; Lohrasbi, S.; Ganji, D.D.; Nsofor, E.C. Simultaneous energy storage and recovery in the triplex-tube heat exchanger with PCM, copper fins and Al_2O_3 nanoparticles. *Energy Convers. Manag.* **2019**, *180*, 949–961. [CrossRef]

107. Shin, D.; Banerjee, D. Enhanced Specific Heat of Silica Nanofluid. *ASME. J. Heat Transfer.* **2011**, *133*, 024501. [CrossRef]

108. Tiznobaik, H.; Shin, D. Enhanced specific heat capacity of high-temperature molten salt-based nanofluids. *Int. J. Heat Mass Transf.* **2013**, *57*, 542–548. [CrossRef]

109. Dudda, B.; Shin, D. Investigation of molten salt nanomaterial as thermal energy storage in concentrated solar power. In Proceedings of the ASME 2012 International Mechanical Engineering Congress & Exposition, IMECE2012, Houston, TX, USA, 9–15 November 2012.

110. Dudda, B.; Shin, D. Effect of nanoparticle dispersion on specific heat capacity of a binary nitrate salt eutectic for concentrated solar power applications. *Int. J. Therm. Sci.* **2013**, *69*, 37–42. [CrossRef]

111. Lu, M.C.; Huang, C.H. Specific heat capacity of molten salt-based alumina nanofluid. *Nanoscale Res. Lett.* **2013**, *8*, 292. [CrossRef]

112. Chieruzzi, M.; Cerritelli, G.F.; Miliozzi, A.; Kenny, J.M. Effect of nanoparticles on heat capacity of nanofluids based on molten salts as PCM for thermal energy storage. *Nanoscale Res. Lett.* **2013**, *8*, 448. [CrossRef]

113. Ho, M.X.; Pan, C. Optimal concentration of alumina nanoparticles in molten Hitec salt to maximize its specific heat capacity. *Int. J. Heat Mass Transf.* **2014**, *70*, 174–184. [CrossRef]

114. Shin, D.; Banerjee, D. Enhancement of specific heat capacity of high-temperature silica-nanofluids synthesized in alkali chloride salt eutectics for solar thermal-energy storage applications. *Int. J. Heat Mass Transf.* **2011**, *54*, 1064–1070. [CrossRef]

115. Shin, D.; Banerjee, D. Experimental investigation of molten salt nanofluid for solar thermal energy application. *ASME/JSME Therm. Eng. Jt. Conf.* **2011**, *38921*, T30024.

116. Likhachev, V.N.; Vinogradov, G.A.; Alymov, M.I. Anomalous heat capacity of nanoparticles. *Phys. Lett. A* **2006**, *357*, 236–239. [CrossRef]

117. Jung, S.; Banerjee, D. A simple analytical model for specific heat of nanofluid with tube shaped and disc shaped nanoparticles. *ASME/JSME Therm. Eng. Jt. Conf.* **2011**, *38921*, T30023.

118. Ebadi, S.; Tasnim, S.H.; Aliabadi, A.A.; Mahmud, S. Geometry and nanoparticle loading effects on the bio-based nano-PCM filled cylindrical thermal energy storage system. *Appl. Therm. Eng.* **2018**, *141*, 724–740. [CrossRef]

119. Chieruzzi, M.; Cerritelli, G.F.; Miliozzi, A.; Kenny, J.M.; Torre, L. Heat capacity of nanofluids for solar energy storage produced by dispersing oxide nanoparticles in nitrate salt mixture directly at high temperature. *Sol. Energy Mater. Sol. Cells* **2017**, *167*, 60–69. [CrossRef]
120. Liu, Y.; Yang, Y. Investigation of specific heat and latent heat enhancement in hydrate salt based TiO_2 nanofluid PCM. *Appl. Therm. Eng.* **2017**, *124*, 533–538. [CrossRef]
121. Wang, F.; Zhang, C.; Liu, J.; Fang, X.; Zhang, Z. Highly stable graphite nanoparticle-dispersed phase change emulsions with little supercooling and high thermal conductivity for cold energy storage. *Appl. Energy* **2017**, *188*, 97–106. [CrossRef]
122. Warzoha, R.J.; Weigand, R.M.; Fleischer, A.S. Temperature-dependent thermal properties of a paraffin PCM embedded with herringbone style graphite nanofibers. *Appl. Energy* **2015**, *137*, 716–725. [CrossRef]
123. Muthoka, M.J.; Xuelai, Z.; Yuyang, Y.; Yue, C.; Xiaofeng, X. Latent heat of fusion prediction for nanofluid based PCM. *Appl. Therm. Eng.* **2018**, *130*, 1590–1597. [CrossRef]
124. Souza, R.R.; Faustino, V.; Gonçalves, I.M.; Moita, A.S.; Bañobre-López, M.; Lima, R. A Review of the Advances and Challenges in Measuring the Thermal Conductivity of Nanofluids. *Nanomaterials* **2022**, *12*, 2526. [CrossRef]
125. Lin, S.C.; Al-Kayiem, H.H. Evaluation of copper nanoparticles—Paraffin wax compositions for solar thermal energy storage. *Sol. Energy* **2016**, *132*, 267–278. [CrossRef]
126. Kannan, P.C.D.; Nadaraj, P. Improving the Efficiency of Solar Flat Plate Solar Collector Using PCM and Nanofluids. *Int. Res. J. Adv. Sci. Hub* **2020**, *11*, 14.
127. Hasan, A.; McCormack, S.J.; Huang, M.J.; Norton, B. Evaluation of PCMs for thermal regulation enhancement of building integrated photovoltaics. *Sol. Energy* **2010**, *84*, 1601–1612. [CrossRef]
128. Chow, T.T.; Pei, G.; Fong, K.F.; Lin, Z.; Chan, A.L.S.; Ji, J. Energy and exergy analysis of photovoltaic-thermal collector with and without glass cover. *Appl. Energy* **2009**, *86*, 310–316. [CrossRef]
129. Hu, C.; White, R.M. *Solar Cells from Basic to Advanced Systems*; McGraw-Hill: New York, NY, USA, 1983.
130. Kumar, R.; Rosen, M.A. Performance evaluation of a double pass PV/T solar air heater with and without fins. *Appl. Therm. Eng.* **2011**, *31*, 1402–1410. [CrossRef]
131. Bejan, A. *Entropy Generation Minimization*; Wiley: New York, NY, USA, 1982.
132. Petela, R. Energy of heat radiation. *Heat Transf.* **1964**, *86*, 187–192. [CrossRef]
133. Nada, S.A.; El-Nagar, D.H. Possibility of using PCMs in temperature control and performance enhancements of free stand and building integrated PV modules. *Renew. Energy* **2018**, *127*, 630–641. [CrossRef]
134. Al-Waeli, A.H.A.; Sopian, K.; Chaichan, M.T.; Kazem, H.A.; Ibrahim, A.; Mat, S.; Ruslan, M.H. Evaluation of the Nanofluid and Nano-PCM Based Photovoltaic Thermal (PVT) System: An Experimental Study. *Energy Convers. Manag.* **2017**, *151*, 693–708. [CrossRef]
135. Sardarabadi, M.; Passandideh-Fard, M.; Maghrebi, M.-J.; Ghazikhani, M. Experimental Study of Using Both ZnO/Water Nanofluid and PCM (PCM) in Photovoltaic Thermal Systems. *Sol. Energy Mater. Sol. Cells* **2017**, *161*, 62–69. [CrossRef]
136. Hosseinzadeh, M.; Sardarabadi, M.; Passandideh-Fard, M. Energy and Exergy Analysis of Nanofluid Based Photovoltaic Thermal System Integrated with PCM. *Energy* **2018**, *147*, 636–647. [CrossRef]
137. Hassan, A.; Wahab, A.; Qasim, M.A.; Janjua, M.M.; Ali, M.A.; Ali, H.M.; Jadoon, T.R.; Ali, E.; Raza, A.; Javaid, N. Thermal Management and Uniform Temperature Regulation of Photovoltaic Modules Using Hybrid PCMs-Nanofluids System. *Renew. Energy* **2020**, *145*, 282–293. [CrossRef]
138. Al-Waeli, A.H.A.; Sopian, K.; Kazem, H.A.; Yousif, J.H.; Chaichan, M.T.; Ibrahim, A.; Mat, S.; Ruslan, M.H. Comparison of prediction methods of PV/T nanofluid and nano-PCM system using a measured dataset and artificial neural network. *Sol. Energy* **2018**, *162*, 378–396. [CrossRef]
139. Sarafraz, M.M.; Safaei, M.R.; Leon, A.S.; Tlili, I.; Alkanhal, T.A.; Tian, Z.; Goodarzi, M.; Arjomandi, M. Experimental Investigation on Thermal Performance of a PV/T-PCM (Photovoltaic/Thermal) System Cooling with a PCM and Nanofluid. *Energies* **2019**, *12*, 1–16. [CrossRef]
140. Al-Waeli, A.H.A.; Kazem, H.A.; Yousif, J.H.; Chaichan, M.T.; Sopian, K. Mathematical and neural network modeling for predicting and analyzing of nanofluid-nano PCM photovoltaic thermal systems performance. *Renew. Energy* **2020**, *145*, 963–980. [CrossRef]
141. Al-Waeli, A.H.A.; Sopian, K.; Yousif, J.H.; Kazem, H.A.; Boland, J.; Chaichan, M.T. Artificial neural network modeling and analysis of photovoltaic/thermal system based on the experimental study. *Energy Convers. Manag.* **2019**, *186*, 368–379. [CrossRef]
142. Al-Waeli, A.H.A.; Chaichan, M.T.; Sopian, K.; Kazem, H.A.; Mahood, H.B.; Khadom, A.A. Modeling and experimental validation of a PVT system using nanofluid coolant and nano-PCM. *Sol. Energy* **2019**, *177*, 178–191. [CrossRef]
143. Sardarabadi, M.; Passandideh-Fard, M.; Heris, S.Z. Experimental investigation of the effects of silica/water nanofluid on PV/T (photovoltaic thermal units). *Energy* **2014**, *66*, 264–272. [CrossRef]
144. Al-Waeli, A.H.A.; Chaichan, M.T.; Kazem, H.A.; Sopian, K.; Safaei, J. Numerical study on the effect of operating nanofluids of photovoltaic thermal system (PV/T) on the convective heat transfer. *Case Stud. Therm. Eng.* **2018**, *12*, 405–413. [CrossRef]
145. Naghdbishi, A.; Yazdi, M.E.; Akbari, G. Experimental Investigation of the Effect of Multi-Wall Carbon Nanotube—Water/Glycol Based Nanofluids on a PVT System Integrated with PCM-Covered Collector. *Appl. Therm. Eng.* **2020**, *178*, 115556. [CrossRef]
146. Salari, A.; Kazemian, A.; Ma, T.; Hakkaki-Fard, A.; Peng, J. Nanofluid based photovoltaic thermal systems integrated with PCMs: Numerical simulation and thermodynamic analysis. *Energy Convers. Manag.* **2020**, *205*, 112384. [CrossRef]

147. Abdelrahman, H.; Wahba, M.; Refaey, H.; Moawad, M.; Berbish, N. Performance enhancement of photovoltaic cells by changing configuration and using PCM (RT35HC) with nanoparticles Al$_2$O$_3$. *Sol. Energy* **2019**, *177*, 665–671. [CrossRef]
148. Abdollahi, N.; Rahimi, M. Potential of Water Natural Circulation Coupled with Nano-Enhanced PCM for PV Module Cooling. *Renew. Energy* **2020**, *147*, 302–309. [CrossRef]
149. Lari, M.O.; Sahin, A.Z. Effect of retrofitting a silver/water nanofluid-based photovoltaic/thermal (PV/T) system with a PCM-thermal battery for residential applications. *Renew. Energy* **2018**, *122*, 98–107. [CrossRef]